Modelling the long term impact of residential heat pump market penetration on the low voltage electricity network

van Eerd, Arend A.

Award date:
2022

Electrical Energy Systems
Department of Electrical Engineering
De Zaale, 5612 AJ Eindhoven
P.O. Box 513, 5600 MB Eindhoven
The Netherlands
www.tue.nl

Author:
Arend van Eerd

Student ID:
0955584

Supervisors:
Prof. dr. ir. J.G. Slootweg (TU/e)
ir. G.G.D. Rouwhorst (TU/e)
ir. J. Reinders (Enexis)

Date
09-05-2022

Modelling the long term impact of residential heat pump market penetration on the low voltage electricity network

Master Thesis

Master program:	Sustainable Energy Technology
Department:	Mechanical Engineering
Research group:	Electrical Energy Systems
Examination committee:	prof. dr. ir. J.G. Slootweg
	dr. ir. J. Morren
	dr. ir. C.M. Rindt
	ir. G.G.D. Rouwhorst

Where innovation starts

TU/e EINDHOVEN UNIVERSITY OF TECHNOLOGY

Declaration concerning the TU/e Code of Scientific Conduct for the Master's thesis

I have read the TU/e Code of Scientific Conduct[1].

I hereby declare that my Master's thesis has been carried out in accordance with the rules of the TU/e Code of Scientific Conduct

Date

5-5-2022

Name

Arend van Eerd

ID-number

0955584

Signature

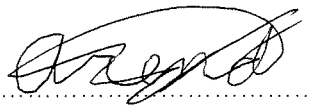

Submit the signed declaration to the student administration of your department.

[1] See: https://www.tue.nl/en/our-university/about-the-university/organization/integrity/scientific-integrity/
The Netherlands Code of Conduct for Scientific Integrity, endorsed by 6 umbrella organizations, including the VSNU, can be found here also. More information about scientific integrity is published on the websites of TU/e and VSNU

Decarbonizing the Dutch energy supply is essential in addressing the growing concerns of climate change. Heating is the largest end-use of energy in most countries. In the Netherlands, heating comprises almost 80% of domestic energy consumption and most of it is done with natural gas. Heat pumps are seen as an important technology capable of reducing or even eliminating domestic natural gas consumption, thus facilitating the electrification of our heat supply. This however approximately doubles the electricity use of households, placing an increasingly high burden on an already congested electricity network. In this study, a model is developed which is capable of generating heat pump load profiles which are used to evaluate what the effects of various degrees of heat pump market penetration will be on medium to low voltage transformers in the coming decade. The model uses a building classification scheme for which the Dutch building stock is divided into size use and age classes. Thermodynamic properties of common building materials are used to generate a 4R3C building model. The building model is then coupled to a heat pump. Various heat pump operating strategies are considered and their load profiles are validated with measured heat pump data. A case study is performed in den Bosch to investigate what various degrees of heat pump market penetration will do on transformer loading. Domestic gas consumption data is used to determine what shape parameters are required for a representative 4R3C building model to have the same annual thermal demand. Electric mobility was also included in the simulation. From the simulation results, three conclusions could be drawn. First, drastic measurements are required to facilitate the electrification of both heating and mobility because it is expected that 46% of transformers will critically overload. Second, this is scenario independent. There was not a single transformer that went from not overloading in the expected scenario to critical overloading in the extreme scenario. Lastly, if electric mobility is not considered, none of the selected transformers critically overload in the expected scenario.

Contents

Contents iv

Acronyms v

List of Figures vi

List of Tables 1

1 Introduction 2
- 1.1 Project background . . . 2
- 1.2 Problem definition and RQ . . . 2
- 1.3 Research question . . . 3
- 1.4 Scope . . . 4
- 1.5 Thesis outline . . . 4

2 System overview 6

3 Heat demand model 8
- 3.1 Heat transfer phenomena in a building . . . 8
  - 3.1.1 Conduction and convection . . . 8
  - 3.1.2 Ventilation and infiltration . . . 9
  - 3.1.3 Solar irradiance . . . 10
- 3.2 4R3C building thermal analogy . . . 11
- 3.3 Domestic hot water . . . 13
- 3.4 Building classification . . . 15
- 3.5 Annual heat consumption using heating degree days . . . 16

4 Heat pump models 19
- 4.1 Working principles of heat pumps . . . 19
  - 4.1.1 Types of heat pumps . . . 20
- 4.2 Coefficient of Performance . . . 21
- 4.3 Tap water heating . . . 22
- 4.4 Control strategies . . . 23
  - 4.4.1 (Floating) hysteresis . . . 23
  - 4.4.2 Degree minute method . . . 24
  - 4.4.3 Multiple hysteresis . . . 25
  - 4.4.4 PID control . . . 25
- 4.5 Tuning PID control . . . 27
  - 4.5.1 Tuning PID control for underfloor heating . . . 27
- 4.6 Hybrid heat pumps . . . 30
- 4.7 Sizing of heat pump and buffer tank . . . 31
  - 4.7.1 Sizing of buffer tank . . . 31

5 Validation of synthetic profiles **33**
5.1 Visual comparison 34

6 Case study: Den Bosch **37**
6.1 Selecting representative buildings for simulation 40
6.2 Impact of other trends in the electricity grid 41
6.3 Scenario's 43
6.4 Results 43

7 Conclusions and discussion **46**
7.1 Discussion and limitations 47

Bibliography **49**

Appendix **51**

A Model assumptions **52**

B Additional case study details **53**
B.1 Additional results and details 53
B.2 Statistics 56

Acronyms

ACH Air Changes per Hour.

API Application programming interface.

ASHP Air Source Heat Pump.

BAG Basisregistratie Adressen en Gebouwen.

BEM Building Energy Modelling.

CoP Coefficient of Performance.

DHW Domestic Hot Water.

DNI Direct Normal Irradiation.

EV Electric Vehicle.

GSHP Ground source Heat Pump.

HDD Heating Degree Days.

HHP Hybrid Heat Pump.

HP Heat Pump.

NZEB Near Zero Energy Building.

P Proportional.

PI Proportional Integral.

PID Proportional Integral Derivative.

SFH Single family home.

TABULA Typology Approach for Building Stock Energy Assessment.

TH Terraced house.

TMY Typical Meteorological Year.

VSHP Variable Speed Heat Pump.

List of Figures

2.1 Exemplary layout of a residential heat pump system. Adapted from: [14] 6

3.1 Heat flow trough wall. Y-axis is temperature. 9
3.2 An illustration of solar angles. 10
3.3 Series and parallel thermal resistances illustrated. 11
3.4 A house and all the elements that contribute to heat generation and transfer illustrated Figure 3.4a and the corresponding thermal network representation Figure 3.4b. 12
3.5 Mean daily draw offs, total annual draw offs, daily probability distribution of events and an exemplary load profile. This is based on a 200 l/day draw off which corresponds roughly to a 4 person US household. According to ENECO, a Dutch energy company, the Domestic Hot Water (DHW) consumption is around 137 liter per day. Figures presented by [20]. 14
3.6 Heating Degree Days visualised with a base temperature of 18°C. 17

4.2 Main differential features of residential heat pump systems. Below the dotted has been implemented in this research. Figure adapted from [14] 21
4.3 Caption 22
4.4 Heating curve according to Equation 4.3 with various radiator exponents. 24
4.5 Variants of 2 stage hysteresis control as proposed by [13]. 25
4.6 Schematic drawing of the working of a Proportional Integral Derivative (PID) control loop. 26
4.7 Impact of Kp and T_{i} on performance of PI controller of the form 4.7 27
4.8 Effects of varying Kp and Ti on settling time for the floor temperature. A base of $K_{\mathrm{p}} = 10.000$ and $T_{\mathrm{i}} = 10.000s$ have been used. 29
4.9 Response of power and indoor temperatures on a tuned underfloor heating controller where the red line on the bottom figure is the power output of the underfloor heating system. As the outdoor temperature fluctuates the power output of the controller responds accordingly minimizing the temperature fluctuation in the room. Tz: zonal temperature, Tm: temperature of the internal structure, Tf: temperature of the floor, Ta: ambient temperature 29
4.10 Space heat demand of buildings met by various sources in a hybrid heat pump. Dark green: natural gas, light green: heat pump, yellow: solar radiation. Black dots: gas usage, blue dots: electricity consumption. At extremely low temperatures the heat output of the heat pump seems to increase. This is a statistical fluctuation in measurements due to the very limited amount of measurements available at these temperatures and will for this research be regarded as zero. Measurements done by [18] 30

5.1 Single heat pump comparison for multiple control strategies. 35
5.3 Same as Figure 5.2 but with nighttime setback temperatures. 35
5.2 Mean of aggregated profiles. 30 synthetically generated, and mean of 30 sample profiles in the datasets. 36

6.1 Skewed normal distribution fit for the annual gas consumption. Skewness = 6.0, loc = 676, scale = 1260. The distribution is highly positively skewed since gas usage is always positive. 39
6.3 Skewed normal distribution fit for the annual gas consumption of 9 of the transformers included in the study in den Bosch. All distributions are highly positively skewed since gas usage is always positive. The K-S test results can be found in Table B.3 40
6.4 Effect of a 20% increase in parameters for all Single family homes (SFHs) and Terraced houses (THs) in the Typology Approach for Building Stock Energy Assessment (TABULA) dataset. The insulation surcharge is defined as an increase in the wall, window, and roof insulation with disregard for the airtightness factor. . . 41
6.5 Inputs and outputs of emobpy and sequence of generating time series [16]. 42
6.6 Power loading of all transformers. The simulation was done for the entire month of January and February. A snapshot of 29th of January to 2nd of February 12:00 is shown because this was a fairly congested period when the simulation was executed. 44

7.1 Actual and theoretical average gas consumption (m3) in dwellings per label category with ±1 standard deviation 48

B.1 Power loading of all transformers with heat pumps but no Electric Vehicle. The simulation was done for the entire month of January and February. A snapshot of 29th of January to 2nd of February 12:00 is shown because this was a fairly congested period when the simulation was executed. 54
B.2 Example of losses that a Volkswagen ID3 experiences in January. 55

List of Tables

3.1 Reference conditions DHW profiles. How tater temperature is 40 °C 15
3.2 Energy label cutoff values in $kWh/m^2/year$ 17

4.1 FL running hours 31

5.1 Controllers present in validation 33
5.2 Boundaries 33
5.3 Setback conditions. 35

6.1 Example of a set of generated representative buildings. 41
6.2 Scenario's that might occur in den Bosch 43
6.3 Number of hours each transformer loading exceeds maximum loading during simulation period with an Electric Vehicle (EV) penetration of 25%. 45

A.1 Assumptions for the building, heat pump and simulation 52

B.1 Number of hours each transformer loading exceeds maximum loading during simulation period without EVs. 53
B.2 Maximum overload of transformers during simulation period. Because this is a single peak during a period of 2 months this value should not be read on its own to draw conclusions. Transformer 79.303 for example has a peak loading in the expected scenario than in the electric scenario (with EV). The overloading Table 6.3 however shows that this transformers critically overloading duration is almost twice as high. 55
B.3 KS statistics of the transformers seen in figure 6.3. Location of the results matches the location of the sub figures. 56

Chapter 1

Introduction

1.1 Project background

On may 20th 2019 the Dutch government laid down the climate act which outlines the Dutch climate strategy. The goal of this plan is to reduce Dutch Greenhouse gas emissions (GHG) by 49% compared to 1990 levels by 2030. Plans are to reduce them by 95% by 2050. The policy measurements to achieve these goals are outlined in the climate plan, the National Energy and Climate Plan (NECP) and the national climate agreement [17]. The National climate agreement contains agreements on sectors on what they will do to mitigate anthropological climate change. The participating sectors are electricity, industry, built environment, traffic and transport, and agriculture [17].

The residential sector is responsible for around 17% of global CO_2 emissions globally. In residential Dutch buildings, the relative heat demand is around 80% of the total residential energy consumption. Currently, this demand is met for about 90% with low caloric natural gas, which has traditionally been widely available in the Netherlands because of drilling operations in the Slochteren gas field in Groningen. However, with the Dutch government's new climate ambitions on CO^2 reductions, as well as the political pressure to reduce the amount of natural gas extraction and imports, alternatives are being investigated. Alternatives for natural gas are however limited since it has a high energy density compared to various sources of renewable energy. As a reference, we can compare the wind energy generated annually by Borssele 1-5 to about 1.5 million m^3 of natural gas, while the Dutch annual consumption is about 30 million m^3 annually.

For the built environment the ambitious goal has been set to transform the 7 million homes and 1 million buildings that are currently present in the Netherlands from a moderately well insulation level heated by natural gas, into well-insulated buildings that are heated using a renewable source by 2050. To achieve this the Dutch environmental planning office made a roadmap consisting of 5 strategies and mixes thereof for the transition of low energy heat from fossil fuel-based natural gas, to one based on renewable energy sources. These strategies are outlined in the 'startanalyse voor aardgasvrije buurten'. This analysis was written for municipalities to help them find alternatives for heating that are acceptable. The guiding principles for selecting viable alternatives for natural gas are that a mix of renewable sources should be applied that give rise to the lowest societal costs, and end-user costs. The strategies involve District heating, biomethane, heat pumps, and hydrogen. For hydrogen, some pilots exist but it is unlikely that it will be a significant part of the heating mix in the near future [32]. Biomethane is also pursued, but there is also a high demand from other industries.

1.2 Problem definition and RQ

When a household would switch from gas heating to a full electric heat pump, the annual electricity consumption of that household will approximately double. The efficiency of Air Source Heat Pump

is strongly dependent on the outside temperature, which means that at times when heating is required most, they operate at the lowest efficiency. A numerical study on Italian households has found that the monthly efficiency could be reduced by as much as 17% when the relative humidity is high (>80%) and the outdoor air temperature is in the range 0-6 °C [36]. Most of the electrical infrastructure components currently in use were installed when a lot less electricity was required. Electrical infrastructure components are built to last. [39] estimated transformers have an average life expectancy of around 35 years. In order to locally reinforce the electricity grid transformers could be replaced before the end of their service life. This however takes time because it is a big logistical challenge. Components have to be ordered and delivered, permits have to be granted and highly specialized personnel is required to install them. This might take years of careful planning and scheduling. It is therefore highly desirable to be able to accurately predict what the impact of electrification trends will be on transformers. This should be done on the transformer level so it can be identified what transformers are most at risk of overloading. This helps to prioritize investments and reduces uncertainty.

Currently, Enexis uses software models in ENET to predict what scenarios and technologies will affect the electricity grid to what extent in peak periods of demand in specific areas. This tool is used to provide local governments with numbers and figures that provide insight into the effects of various heat strategies. The heat pump load profiles that are used in the calculations are based on raw data from the measurements in the Your Energy Moment project [8]. This dataset contains measurements of 37 heat pumps with 15-minute load intervals for an entire year with the corresponding outside temperature. The heat pumps were identical two-stage heat pumps with a 1 kW space heating and a 1.8 kW hot tap water output. The effect of both types of operation could be separated since the heat pumps were of type on/off. This means that if a load of 1 kW is measured space heating was turned on and if a load of 1.8 kW was measured tap water was heated. Additionally, simultaneity could be modeled since 37 units were present in the dataset.

To achieve a better understanding of how when and where problems will occur in the electricity grid the effect of various types of heat pumps must be modeled more precisely. In order to do this research needs to be done on the various types of heat pumps and their grid impact. For example, the hybrid heat pump is expected to play a major role in the transition from all-natural gas to a fully electric low heating supply [4]. In older buildings with low to medium insulation standards, the heat demand in cold winter periods is substantial. This coincides with low efficiency for air source heat pumps and such a heat pump might not be able to meet the heating demand [34]. Additionally, the installation of heat pumps requires low-temperature radiators or underfloor heating. When both are not present in a building the costs for hybrid heat pumps are considerably lower (around 25% compared to air-source heat pumps) making it an attractive option for many homeowners that do not have underfloor heating [4]. Other actors such as netbeheer Nederland recently released a statement advocating for the widespread adoption of hybrid heat pumps with a call to install 1-2 million hybrid heat pumps before 2030 [30].

1.3 Research question

Underpinning this issue the following research question and sub-questions will be defined:
How can the impact of residential heat pump market penetration on low to medium voltage transformers be modeled?

1. How can the characteristics of a building be used to model its heat demand? *chapter 3*
2. How can this model be generalised so a variety of Dutch buildings can be simulated? *chapter 3* & *chapter 6*
3. What are the various types of heat pumps, how can they be characterized, and how can they be modeled? *chapter 4*
4. How are heat pumps controlled and what is the impact of various control strategies on their load profiles? *chapter 4* & *chapter 5*

5. What is the effect of the adoption of heat pumps on Dutch low to medium voltage transformers? *chapter 6*

1.4 Scope

To keep the scope of the project within reasonable bounds, the following elements are within the scope of this research:

Components: The impact analysis will be done on the medium voltage transformer level, other network components are out of scope

Time boundaries: The horizon for the analysis is 2030.

Type of installations: Installations are installed on the low voltage network and focus only on the individual consumer level. Community shared initiatives (such as a collective heat pump or heat grid are out of scope).

Loading type: The analysis is done on the demand side of electricity. Production as a result of decentralised electricity generation is not taken into account.

Outside of scope:

Demand-side management: Demand-side management offers great potential for network operators to shift some of the peak loadings to less congested moments in time. However with many uncertainties concerning when, where, and how it is still unclear how this will be implemented. While the model developed will be flexible enough to accommodate such control strategies, it is not taken into account in the case study.

Low and high voltage networks: LV networks are simulated as an aggregated load and the high voltage network is modeled as an infinite ideal bus.

Voltage constraints: Voltage constraints are not considered and are considered out of scope. This depends on the specific network configurations and is therefore not taken into account. Additionally, voltage network constraints are usually not an issue on the demand side, because this has historically been taken into account in transformers.

Short-term forecasting, and short-term behavior: The measurement interval is 15 minutes and the prediction horizon is around 10 years.

1.5 Thesis outline

chapter 2 sketches a complete picture of how all parts of a heat pump system with heat distribution and tap water are connected. This is used as the basis for modeling the system and explaining how all components interact.

chapter 3 explains how the mechanisms of heat transfer in a building work. It introduces all thermal losses to the environment and also states the sources of heat gain. It continues to formulate this in a mathematical model which can be used for simulation purposes. Furthermore, it explains how Domestic Hot Water load profiles are generated. It also introduces a building classification scheme that enables the grouping of a large variety of Dutch buildings. This makes the heat demand model widely applicable. Furthermore, it introduces a method to use the heat demand model to calculate annual thermal load without running a full-year simulation. This is later used to compare synthetically generated buildings to real-world buildings.

chapter 4 begins by explaining the general theory of how heat pumps work and on what dimensions they are distinguished. It continues by formulating the control strategies of both single-speed and variable-speed heat pumps. These control strategies are also mathematically described. It also

formulates how a Hybrid Heat Pump model is implemented. Furthermore provides a general rule for the sizing of a heat pump so the correct heat pump size can be chosen for a specific building.

chapter 5 compares simulated heat pump load profiles with measured heat pump load profiles for verification purposes. Three validations will be done. Operation of a single heat pump, a combined load profile, and a combined load profile with nighttime setback temperatures.

chapter 6 combines all the models that have been developed to study the impact of heat pump market penetration on transformers in 's Hertogenbosch in a scenario-based manner. Statistical analysis of dwelling gas consumption measurements is done to make accurate distributions of building thermal demand. These distributions are transformer specific, which allows differentiation between rural and urban areas, resulting in more accurate predictions. These thermal demands are combined with the building classification scheme, the building model, and the heat pump model to generate transformer-specific heat pump load profiles. Electric Vehicle adoption is also taken into account.

Finally chapter 7 concludes the sub-questions and presents the main conclusions of the project. The limitations of this research are also discussed.

5 Modelling the long term impact of residential heat pump market penetration on the low voltage electricity network

Chapter 2

System overview

The impact of heat pumps on transformer loading will be modelled by generating heat pump electricity load profiles and adding them to current transformer power loading. This is compared to the maximum load that a specific transformer can handle to make predictions of what the impact of various degrees of heat pump market penetration will be on specific transformers. This is done in a scenario base manner so a range of various predictions can be considered. When doing this the amount and the type of buildings that are connected to a specific transformer are taken into account as to make transformer specific predictions.

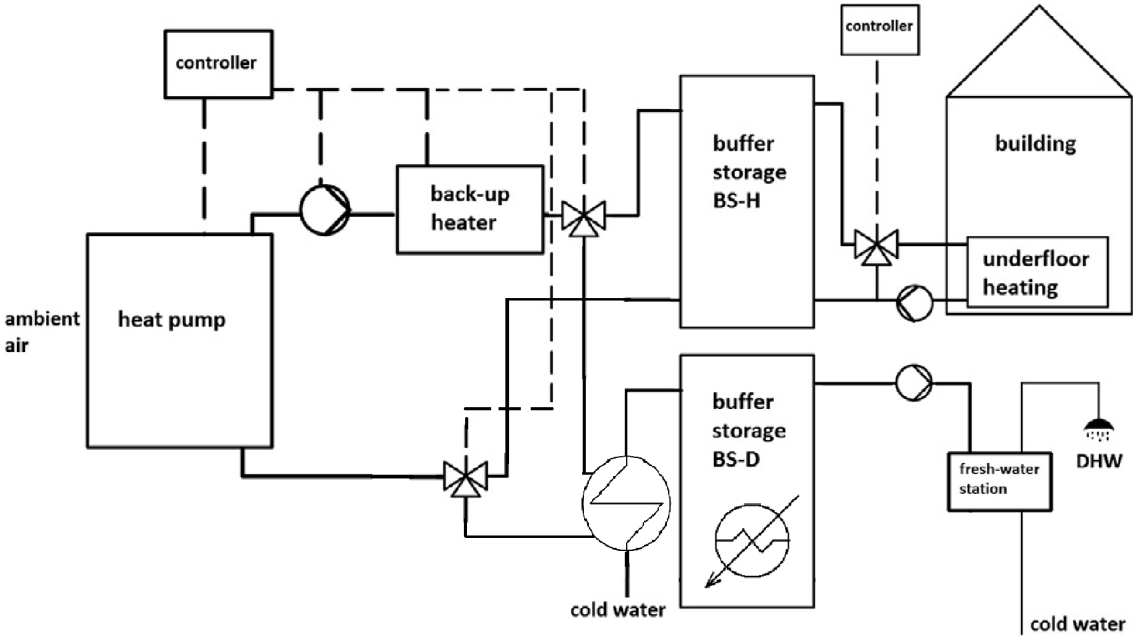

Figure 2.1: Exemplary layout of a residential heat pump system. Adapted from: [14]

To generate heat pump load profiles a bottom up approach is taken for which a system model is made. Figure 2.1 displays the generalised system is model. A building is heated via an underfloor heating system that is installed on every room and on every floor except the attic. During the heating season the building looses thermal energy to the environment which cools down the building. The way this happens is explained in chapter 3. Because of this cooling effect the indoor temperature drops below the set point temperature of the thermostat, which is set at 20°C, [26]. This sends a message to the underfloor heating controller which adjusts the temperature of the water that flows through the floor. How this controller is modelled is explained in subsection 4.5.1.

The underfloor heating are a set of pipes placed in a spiral configuration which are poured in concrete in the floor. Through these pipes warm water flows at a constant flow rate that heats up the rooms. The pipes are connected to a manifold which is connected to a 3-way valve. The three way valve regulates how much of the underfloor heating water remains in the loop and how much is replaced with new hot water from the space heating buffer tank. If the controller detects that heating is required it sends a signal to the three way valve to open the valve slightly more so more hot water enters the system. It is the controllers responsibility to make minimal adjustments to the valve so the heat demand is balanced as much as possible with the heat supply.

The space heating buffer tank is heated from the heat pump and potentially a backup heater (more on this in subsection 4.1.1). The bottom of the tank, which contains the coldest water is connected with a three way valve to the ensure the cold water goes to the heat pump for heating. Here two variants can be made. The first is where DHW is preheated by the heat pump, this is shown in Figure 2.1. Hot water that exits the heat pump is split by a three way valve to go to the buffer storage heating tank, and part to a heat exchanger. In this heat exchanger cold tap water (assumed year round to be 15 degrees) is preheated from the heat pump. It then enters a buffer storage tank where its heat is boosted to around 60°C to prevent legionella bacteria (more on this in section 4.3). When hot tap water is required for activities such as taking a shower it is first mixed with colder water so it reaches a temperature of 40 °C, which is the consumption temperature of DHW. The other strategy could be that all the DHW needs are met by electric resistance heating. In this case the heat exchanger is not present.

The cold water returns to the heat pump where it is heated. The working of this is explained in chapter 4. Modelling of the controller is explained in section 4.4. The literature review indicated that a variety of controllers are used in literature, but comparing what the impact of various controller strategies on heat pump profiles is is not covered much in literature.

Various variation in buildings, heat pumps and heat pump operating strategies are simulated to generate load profiles that could be present in the Enexis network. Adding these to current transformer loading during the winter period is done to make predictions for what network assets need reinforcement in the coming decade.

Chapter 3

Heat demand model

In this chapter, the method for determining the instantaneous demand for the heat of a building is explained. The demand for heat is split between space heating and the use of hot water for activities such as showering. For space heating the following phenomena will be considered:

- Conductive and convective heat losses
- Ventilation and infiltration heat losses
- Solar irradiation gains
- Internal heat gains from various activities (e.g. humans emitting heat, cooking, computers)

It is also assumed that all heating is done through an aquatic underfloor heating system which is connected to a buffer tank on all floors. The floor is assumed to be a 10cm thick concrete slab on all floors. For details of the properties of the underfloor heating system see Table A.1

3.1 Heat transfer phenomena in a building

3.1.1 Conduction and convection

Conduction is defined as the diffusion of thermal energy within one material or between materials that contact each other. This occurs because the object with the higher temperature has molecules that vibrate with more kinetic energy. The collisions that occur between these molecules distribute the kinetic energy thus transferring it. Inside or between solid materials conduction is the main mode of heat transfer.

convection is a heat transfer mechanism within a fluid or at the interface between a fluid and a solid. Convection is driven by the motion of the fluid. This happens even when the fluid is not blown by an external force such as wind. The part of the fluid that contacts a hot surface heats up, this decreases its density locally which makes it rise while the denser, colder portion of the fluid sinks. This process repeats itself because the less dense fluid cools as it moves away from the heat source which makes it sink again. Similarly, the cold fluid is now in contact with the heat source thus it warms up. This process creates natural circular convection currents. On a global scale, this process is responsible for wind currents while indoors it circulates heat through a building and to the walls. A distinction is made between natural convection: the process described before, and forced convection: a situation where air currents are forced by an external force such as a fan.

The time derivative of the first law of thermodynamics states that the change in internal energy (U) of a system is equal to the amount of heat (Q) added to the system minus the work done (W) by the system Equation 3.1. The change in internal energy is defined in Equation 3.2. Since there is no work done by or to the building this term becomes 0 and the heat flux becomes equal to the change in internal energy. In Equation 3.2 m is the mass of the medium and C is the heat capacity of the medium.

$$\frac{dU}{dt} = \frac{dQ}{dt} - \frac{dW}{dt} \tag{3.1}$$

$$\frac{dU}{dt} = mC\frac{dT}{dt} \tag{3.2}$$

The method of heat transfer from indoors to the outdoor environment (given the temperature inside is higher than outside) is illustrated in Figure 3.1. First convective heat transfer from the inside air heats the surface of the inner wall. From here conduction takes place through the inner wall, insulation layer, and outside wall. Then convective heat transfer to the outdoor air occurs. The formula for conduction is shown in Equation 3.3. Here k is the thermal conductance of the specific material in $W/(m \cdot K)$, which is a material property, A is the surface area through which conductance occurs in m^2, x is the thickness of the wall in m and ΔT the temperature difference. Convective heat transfer happens according to Equation 3.4 where h is the convective heat transfer coefficient in $W/(m^2 \cdot K)$. This coefficient depends on material properties *as well as fluid velocity.* In free convection this value is between 2.5 and 25 $W/(m^2K)$ [21].

$$\frac{dQ}{dt}_{cond} = kA\frac{\Delta T}{\Delta x} \tag{3.3}$$

$$\frac{dQ}{dt}_{conv} = hA\Delta T \tag{3.4}$$

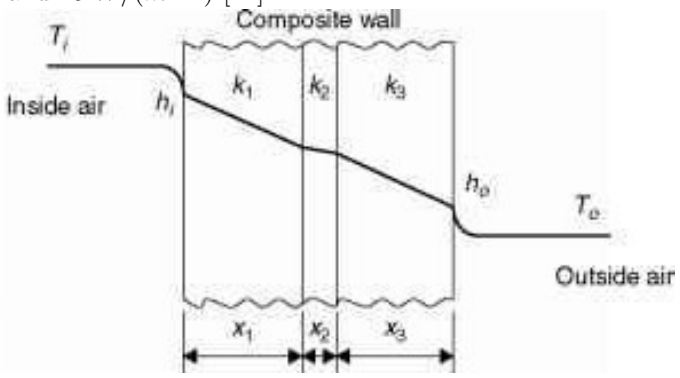

Figure 3.1: Heat flow trough wall. Y-axis is temperature.

The effects of conduction and convection combined are also referred to as transmission.

3.1.2 Ventilation and infiltration

Another important component in heat transfer between the outdoor and indoor environment is mass transfer. If a cold object from the outside is carried inside this will contribute to a heat loss inside the system. The only mass transfer component in buildings that is important in heat transfer calculations is the air exchange with the environment. Buildings are not perfectly sealed entities, and even well-insulated buildings will exchange inside air with the environment. Air exchange with the environment is expressed in Air Changes per Hour (ACH). In well-insulated buildings this is often done on purpose since breathing quality air is essential to human health. ASHRAE, the leading authority on building heating cooling, and ventilation regulations, recommends at least 0.35 ACH per person as the minimum ventilation rate in residential buildings. This value however greatly differs between buildings depending on airtightness, climate, and even occupant behavior (opening windows for example). Further reading will determine upper and lower bound values for different insulation standards to use in the simulation. The formula for ventilation and infiltration heat loss is described by Equation 3.5.

$$\dot{Q}_{vi} = (1-\beta)\frac{c_{air} * \rho_{air} * V_{building} * ACH * \Delta T}{3600} \tag{3.5}$$

Where $\dot{Q}_{vi} = dQ_{vi}/dt$ is the infiltration or ventilation heat loss per second, c_p is the heat capacity of air, ρ is the density of air, $V_{building}$ is the combined volumes of the heated rooms, ΔT the temperature difference between the inside and outside air, β is the efficiency of the heat recovery system (0 for infiltration) and ACH is the Air Changes per Hour of the heat loss mechanism in question.

In modern very well insulated buildings infiltration rates are often below 0.35 ACH and mechanical ventilation is required for occupants' health. This is often combined with heat recovery

9 Modelling the long term impact of residential heat pump market penetration on the low voltage electricity network

ventilation. This limits the heat loss through ventilation. Heat recovery in ventilation is often done in newly built buildings but seldom seen in older homes. For this research, a variety of heat recovery systems have been used depending on the building typology section 3.4

3.1.3 Solar irradiance

Solar irradiance can contribute to high heat gains in the summer, but even quite some heating savings during the fall, winter and spring. Heat gains by solar radiation come from Direct Normal Irradiation (DNI): the radiation that directly hits the building, and indirect radiation. Radiation that first hit other surfaces and is re-radiated and then hits the building. For this research, only radiation that enters through windows is taken into account. Solar radiation that heats the outer walls is ignored.

In Figure 3.2 it can be seen how solar energy heats a window. From this figure, the solar intensities for each wall (North, East, South, West) can be deduced to Equation 3.6. Here I_x are the Direct Normal Irradiation (DNI) of solar radiation on the windows of the corresponding walls, I the intensity of solar radiation and α_b is the azimuth angle of the building. The intensity of solar energy is never below 0. In the formula for the angle, this would mean the solar energy is on the opposite wall (e.g. North instead of South). In practice, this would mean no energy from that angle, not negative energy.

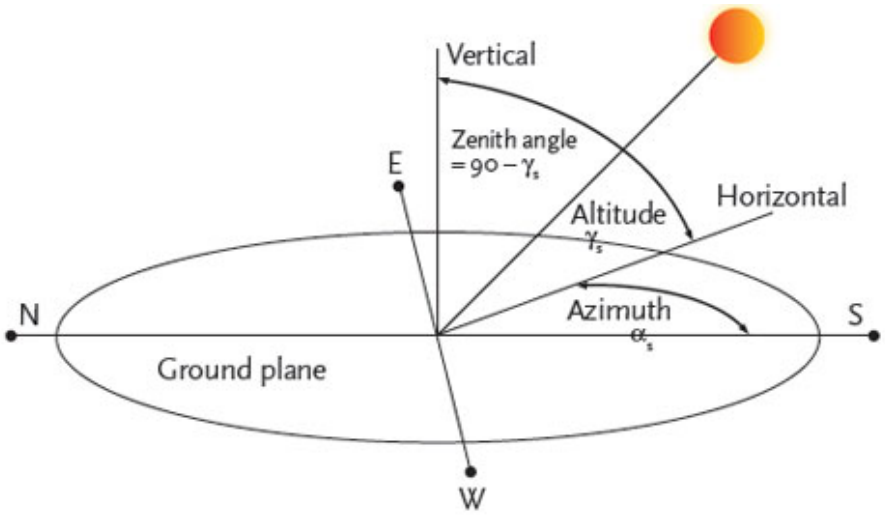

Figure 3.2: An illustration of solar angles.

$$\begin{bmatrix} I_N \\ I_E \\ I_S \\ I_W \end{bmatrix} = I \cdot \begin{bmatrix} A_N \\ A_E \\ A_S \\ A_W \end{bmatrix} \cdot \begin{bmatrix} max(0, \cos(\alpha_s - \alpha_b)) \\ max(0, \sin(\alpha_s - \alpha_b)) \\ max(0, \cos(\alpha_s - \alpha_b)) \\ max(0, \sin(\alpha_s - \alpha_b)) \end{bmatrix} \cdot \cos \gamma_s \tag{3.6}$$

Solar radiation that hits the windows is either reflected, transmitted, or absorbed. Radiation that is reflected does not heat the building. Radiation that is transmitted enters the building where it heats various surfaces. Radiation that is absorbed heats the window. This energy is then partially transferred to the room and outdoor via convection and partially re-radiated as infrared radiation. Since glass is not transparent to infrared radiation it cannot leave the building and heats it. It is assumed that around 4% of the heat energy that hits the window heats the room via convection or infrared radiation. The amount of energy that impacts the inner surface of the building is expressed in Equation 3.7

$$\dot{Q}_{solar} = sum(I_{sol} \cdot \tau_{window}) \tag{3.7}$$

Where $\dot{Q}_{solar}$ is the total heat flux through all the windows in $[W]$. And τ is the transmittance of the window. This is a property of building materials and thus depends on the type of windows used and different for various buildings present in the simulation section 3.4. It can range from 0.3 to 0.8 [5]

Shading The effect of shading from inside blinds and surrounding buildings has not been taken into account.

3.2 4R3C building thermal analogy

Two systems are said to be analogous to each other if two conditions hold:

- The two systems are physically different
- Differential equation modeling of the systems are the same

This holds for electrical and thermal systems. Heat conduction is similar to the conduction of electrical currents in electrical systems. In an electrical system, the current is driven by potential differences. In thermal systems, heat flow is driven by temperature differences. Representing building elements as thermal resistances greatly simplifies equations. In a planar wall, the formulas for heat transfer can be expressed as seen in Equation 3.3 and Equation 3.10

$$\begin{aligned} \frac{dQ}{dt}_{cond} &= kA\frac{\Delta T}{\Delta x} \\ \dot{Q}_{cond} &= \frac{\Delta T}{R_{cond}}, where \\ R_{cond} &= \frac{\delta x}{kA} \end{aligned} \tag{3.8}$$

$$\begin{aligned} \frac{dQ}{dt}_{conv} &= hA\Delta T \\ \dot{Q}_{conv} &= \frac{\Delta T}{R_{conv}}, where \\ R_{conv} &= \frac{1}{hA} \end{aligned} \tag{3.9}$$

Where $\dot{Q}$ is the heat flux $\frac{dQ}{dt}$ in W and R the thermal resistance in $Kelvin/Watt$

This method allows us to add thermal resistances together and construct a thermal network in a similar manner as is normally done in electrical resistance calculations. In Figure 3.3a and Figure 3.3b it can be seen how series and parallel resistances look like graphically. In a series connection, heat has to go through all sections. For example, when heat has to pass through an inner wall, then a slab of insulation, and then the outer wall. In a parallel connection, the heat flow can take multiple paths simultaneously, such as either a window, a wall, or a door. The formulas for adding these resistances are Equation 3.10

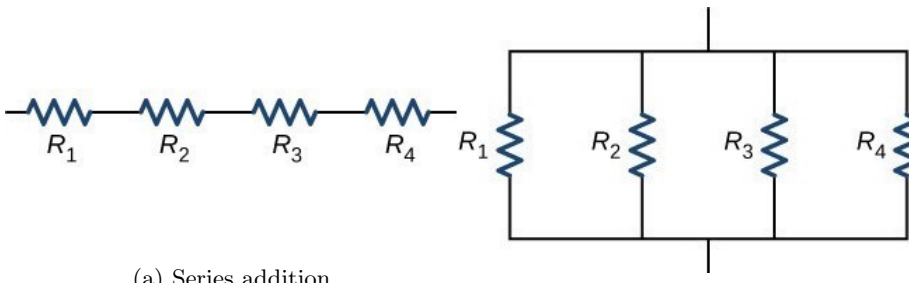

(a) Series addition

(b) Parallel addition

Figure 3.3: Series and parallel thermal resistances illustrated.

$$R_{series,tot} = \sum_n R_n \qquad R_{parallel,tot} = \frac{1}{\sum_n \frac{1}{R_n}} \tag{3.10}$$

And equations 3.8 and 3.9 can be written more generally as 3.11

$$\dot{Q} = \frac{\Delta T}{R} \tag{3.11}$$

With this information, we can construct a thermal network of the building illustrated in Figure 3.4b. First, a schematic drawing is made of the building with all the important components. This is then translated to a thermal network scheme where equations 3.2 and 3.11 can be combined to calculate heat transfer.

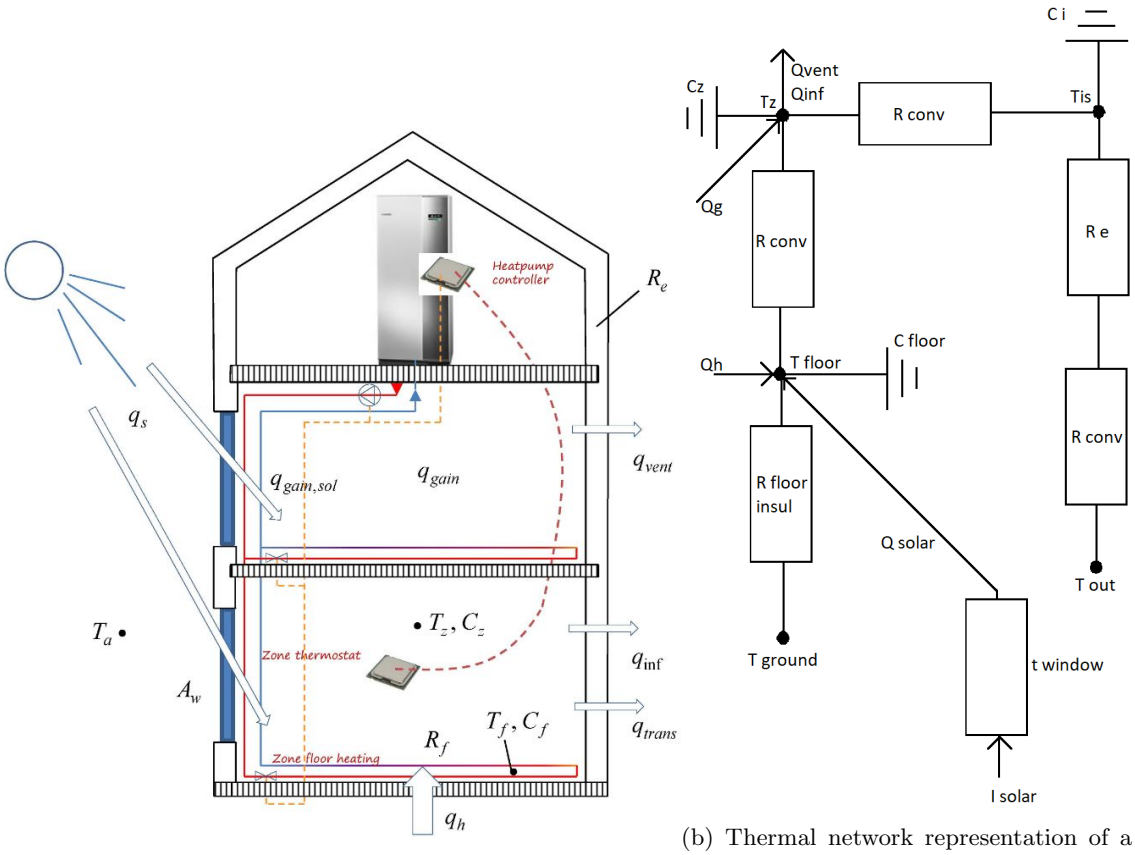

(a) Modelling scheme of a house [24].

(b) Thermal network representation of a house.

Figure 3.4: A house and all the elements that contribute to heat generation and transfer illustrated Figure 3.4a and the corresponding thermal network representation Figure 3.4b.

Here T_{ground}, T_{floor}, T_z, T_{is}, T_{out} are the ground (below insulation slab), floor, zonal, inside building surface (except floor) and outdoor temperature respectively. The C values at these temperature nodes are the corresponding heat capacities.

At the floor node, heat is added from the underfloor heating system. Solar radiation is also absorbed here according to Equation 3.7. The heat added to the floor is transferred to the air in the room via convection, and part of it is conducted to the ground through the insulation under the floor (only for the ground floor). In the zonal temperature node heat is directly absorbed from generated heat by appliances and people. Ventilation and infiltration heat losses are also connected here. Via convection, the inner surfaces of the building are heated, which has a capacitance C_i. R_e is the total conductive thermal resistance of the inner shell (windows, walls, doors, roof) which is computed via parallel thermal resistance addition. On the outer walls, convection is responsible for heat transfer to the environment. The effect of wind velocity is neglected thus the convective heat transfer coefficient of the outside air is assumed to be the same as the inside air. This network allows us to express the heat balance in mathematical formulas.

$$C_f \frac{dT_f}{dt} = \frac{T_z - T_f}{R_{conv}} + \frac{T_g - T_f}{R_{f,insul}} + \dot{Q}_g + \dot{Q}_{sol} \tag{3.12}$$

$$C_z \frac{dT_z}{dt} = \frac{T_f - T_z}{R_{conv}} + \frac{T_{is} - T_z}{R_{conv}} + \dot{Q}_g + \dot{Q}_{irrad} - \dot{Q}_{vent} - \dot{Q}_{inf} \tag{3.13}$$

$$C_{is} \frac{dT_{is}}{dt} = \frac{T_{out} - T_{is}}{R_{conv} + R_e} + \frac{T_z - T_{is}}{R_{conv}} \tag{3.14}$$

Here it is important to note that R_{conv} from the ground to the zone is different than R_{conv} to the inner surface and outer surface. This is because R_{conv} ground to zone is $1/(h \cdot A_{floor})$ and R_{conv} zone to inner surface is $1/(h \cdot A_{is})$. The inner surface is roughly the same as the outer surface therefore R_{conv} zone to inner surface = R_{conv} outer surface - out. This Representation is a 4R3C thermal network since this is the highest reduction possible for this network. If more detail would have been taken into account, such as the outdoor wall temperature, more R and C values could have been combined to construct a higher order network. [24] however showed that increasing the amount of R and C parameters after this level of detail, the model accuracy only marginally increases. To balance model complexity and accuracy a 4R3C network has been chosen.

Internal heat generation is also taken into account. A person in rest generates around 100 W of energy in rest. Additionally, computers, lighting, and other appliances generate a small amount of heat. Cooking generates quite a lot of heat. For this research, a constant of 3 W/m^2 living area is taken in accordance with [25].

The storage tank for space heating and DHW water is modeled as a perfect insulated cylinder. In reality, this is not true and its internal temperature drops slowly. However, the heat that escapes from the storage tanks leaks into the building, so it is not lost. For simplification reasons, this is not modeled.

3.3 Domestic hot water

Apart from space heating building occupants also require Domestic Hot Water (DHW) for various reasons such as showering, bathing cleaning cooking. Contrary to space heating requirements hot water demand depends more on occupant behavior and composition than building typology. It has been estimated that hot water consumption accounts for about 18% of total residential energy consumption in North American homes [31]. Since heat pumps have lower efficiency at higher temperatures and tap water needs to be heated to higher temperatures than space heating water, this number is likely higher when heat pumps are used as heating devices (see section 4.3). Furthermore many people shower in the morning or in the evening which results in a high coincidence factor for hot water consumption. This can put high loads on the electricity grids simultaneously. Space heating has a much lower coincidence factor since it is generally advised against setback temperatures when a heat pump is combined with an underfloor heating system.

[20] realized the importance of stochastic load profiles by measurement data and observations of occupants. They identified a set of 4 classes that can be distinguished in DHW consumption. Short tapping, long tapping, showering, and bathing. They constructed a probability distribution function for those classes that describe the probability of occurrence during the day. An example can be seen in Figure 3.5c.

ENECO, a Dutch energy company, estimates that the mean consumption of DHW is around 137 liter per day. In general 2 effects of the mean daily consumption of DHW throughout the year can be observed. First, the mean daily consumption follows a sinusoidal curve throughout the year. In wintertime people generally take slightly longer hot showers or a bath than in the summer. Some people shower slightly colder or even only cold during the summer months. Furthermore, [19] mentions the holiday season as another cause for reduced consumption. Secondly, there exists a strong stochastic deviation of mean daily consumption during the year. Individuals might not shower for a day or two, and suddenly decide to take a bath. Or a family could be on a weekend

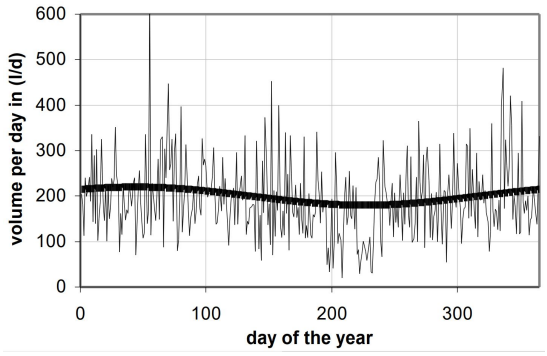

(a) Example of DHW consumption per day throughout the year.

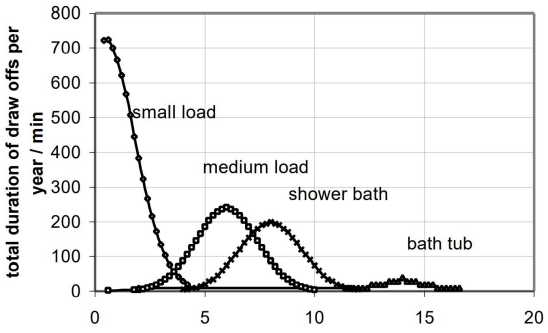

(b) Nr. of draw-offs during one year as a function of the DHW-flow rate.

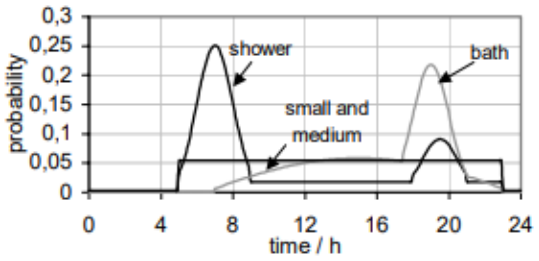

(c) Probability density function throughout the day of water tapping events.

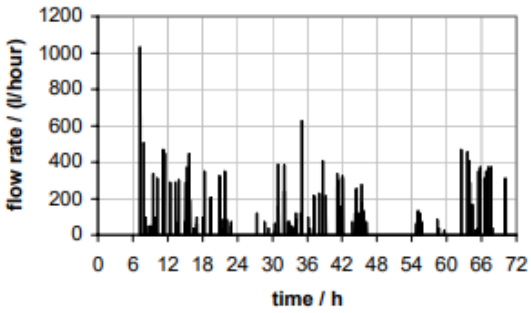

(d) Example of a 3 day profile of hot water consumption.

Figure 3.5: Mean daily draw offs, total annual draw offs, daily probability distribution of events and an exemplary load profile. This is based on a 200 l/day draw off which corresponds roughly to a 4 person US household. According to ENECO, a Dutch energy company, the DHW consumption is around 137 liter per day. Figures presented by [20].

trip thus not using any hot water, but then all take a shower when they are back both these effects can be seen in Figure 3.5a.

Generating stochastic synthetic DHW profiles from events requires two inputs. First the probability of an event occurring which has been explained. The second is the amount of hot water consumed during this activity. The amount of water consumed during an activity is calculated by multiplying the flow rate by the duration of the draw-off. The flow rate is normally distributed and the duration is assumed to be constant throughout the year. In Table 3.1 the mean flow rate and standard deviation for all categories are listed. The amount of inclinations per day is a mean value per year that will vary each day. The portion of usage illustrates the fraction of DHW that is consumed by an activity on an annual basis. These conditions are also graphically illustrated in Figure 3.5b. An example of a synthetically generated profile can be seen in Figure 3.5d.

This method for constructing stochastic DHW consumption profiles has been studied and verified by [37]. They based their input variables on a large-scale European-wide time of use survey from 2008. This survey targeted the resident population of various countries in Europe living in private households. This survey asked everyone in the household being 10 years or older to track all their daily activities on a 10-minute basis in a diary. This diary included the description, duration, and geographic location of the activities. This study covered individuals ranging from 10 to 97 years of age with various family compositions, such as couples, families, and singles living in different rural and urban settings. After filtering the dataset for data completeness a total of 431 persons in 169 households remained for analysis. Based on the survey results the parameters in dhwCalc, a software tool developed by [19] for DHW profile generation, were

determined and profiles generated. The synthetic profiles were compared against two datasets with measurements of electricity and hot water consumption. One was an aggregated set which was done in an apartment complex where a central hot water distribution system was present. The other was done on the household level on 10 detached houses. They concluded that synthetic profiles generated based on time of use survey and probabilities accurately describes temporal and annual consumption profiles [37].

Table 3.1: Reference conditions DHW profiles. How tater temperature is 40 °C

	short	med	bath	shower
mean flow rate [L/min]	1	6	14	8
sigma [L]	2	2	2	2
duration [min]	1	1	10	5
mean inc/day	28	12	once a week	2
portion of usage	0.14	0.36	0.1	0.4

The DHW consumption profiles were generated using the dhw calc software with the settings shown in Table 3.1. The mean daily draw-of rate was set at 137 liters per day, in line with ENECO data. The probability distribution of Figure 3.5c was used with a sinusoidal amplitude of 10% with a peak at the 45th day of the year. These values were chosen according to the values found by [20, 19]

3.4 Building classification

There exists no database that encapsulates all building characteristics of all buildings in the Netherlands. This would be practically impossible and would be subjected to many privacy concerns. For this reason, it is a common approach to compile a set of representative buildings, assess their properties, and use this as an input for simulation purposes. This avoids the knowledge gap problem while still being able to cover a high diversity of buildings. Increasing the number of representative buildings increases the accuracy of the simulation since any given building has a closer match to the representative buildings.

For this research, it has been chosen to use the TABULA web tool database as a source for building classification input and retrieving various building properties. TABULA is the research output of the Energy Performance Indicator Tracking Schemes for the Continuous Optimisation of Refurbishment Processes in European Housing Stocks (EPISCOPE) which is funded by the Intelligent Energy Europe Programme of the European Union. In the framework of the TABULA and EPICSOPE project residential building typologies have been created for 20 European countries. The national topologies are comprised of a classification scheme that groups buildings by age, size, functionality, and further parameters. The thermal properties of all buildings are compared for different age and functionality bands. This has been done by assessing the building materials and their properties that were often used for buildings built at a specific time. From this data, they created a set of syntactical average buildings which are statically representative for specific age and size bands. In the context of inhomogeneous buildings in the European building stocks these averages allow for an understanding of the energy performances and variation of parameters in thermal properties [26]. The Dutch building stock has been summarised by the Delft University of Technology OTB - Research for the built environment.

The differentiation between the following building categories have been made:

1. Single family home (SFH) - a building that is intended for housing one person and her family with the following characteristics.
    - There are no houses above or below this building
    - Access to the building is directly on the public road.
    - It has a living room and 2 or more bedrooms on another floor.

- Here is a cooking area and sanitary facilities that are exclusive to the inhabitants.

2. Terraced house (TH). Same as SFH but placed in a row with two shared walls. The variant of this is the end house which only has one shared wall. With roughly four out of the seven million homes being a TH it is the most common living situation in the Netherlands.

3. Multi-Family House - multiple separate housing units for residential inhabitants are contained within one building or several buildings within one complex [38]. Technically any number of units can be contained within one building, but when more than 5 units are present they become commercial properties in many countries [38]. Units can be owned and rented by occupants.

4. Apartment Block - similar to a multi-family house. Many units are present and it is a commercial property owned by one entity. Occupants rent the apartments.

For each building six generations are defined (0-1965, 1965-1974, 1975-1991, 1992-2005, 2006-2014, 2015-present). In addition, three to four insulation levels are defined. Original insulation consists of typical insulation standards and building materials at the time. Improved standard, is a measure that can be taken and is often economically beneficial in economic terms. These might be standards when individuals renovate (parts of) their home and insulating is a logical choice. Within some buildings, there could exist 2 categories within this scheme. Differentiation is made based on the ease of installation of a heat recovery system, which reduces ventilation losses. The last category is the ambitious standard, or Near Zero Energy Building (NZEB). This standard includes high very high-quality insulation, high air tightness, a balanced heat recovery ventilation system, a heat pump with solar energy, and a solar boiler for DHW. Especially in older buildings, this is very hard to achieve due to the extensive renovation that is required for this standard, but it is possible depending on the situation. Additionally, the TABULA database covers a set of special buildings, such as the portiekflat, maisionetteflat, and more. These will however not be included in this research because they are relatively rare. This results in a total of 72 building variants that are present in the classification scheme.

3.5 Annual heat consumption using heating degree days

To compute the annual energy consumption of a building when all thermal properties are known two approaches can be taken.

1. A detailed annual simulation. This can be done with the thermal model developed in section 3.2, or with a model of the building made in a Building Energy Modelling (BEM) modeling software package such as DesignBuilder Simergy or CityBES.

2. Use Heating Degree Days (HDD) to calculate the annual energy consumption with less computational overhead.

For this research, it is important to assess the annual energy consumption of a building for two reasons. First, this allows the assessment of an energy label. Energy labels of buildings are measured in kWh/m^2 per year. The associated label for a certain heat demand can be seen in Table 3.2. The second reason is that synthetic houses are simulated which are used for transformer load calculations. The annual thermal energy demand of simulated buildings will be compared to the gas usage data of actual buildings. This allows for simulating more realistic buildings without knowing all their physical properties. Doing a detailed annual simulation for each building present is very computational intensive while only a short winter period is required. Therefore the HDD method is applied.

HDD are used in the Netherlands to assess energy labels of buildings when thermal properties are known. This method is standardized in NEN-EN-ISO 15927-6:2007. The theory is that the amount of space heating a building requires is directly proportional to the outdoor temperature. A

Table 3.2: Energy label cutoff values in $kWh/m^2/year$

Label	G	F	E	D	C	B	A	A^+	A^{++}	A^{+++}	A^{++++}
Cutoff value		380	335	290	250	190	160	105	75	50	0

day becomes a heating day when the average outside temperature over a 24-hour period becomes low enough to require heating. These measurements are based on a threshold called the base temperature. In the Netherlands, this temperature is set at 18°C. This temperature is chosen because it is assumed that an average person heats her home to 20 °C. With internal generation from effects described earlier, 18 °C is assumed to be the balance point temperature of an average building (i.e. the temperature outside for which no extra internal heating is required).

For a heating day, the temperature difference between the base temperature and the actual temperature is summed over the hours if the temperature is lower than the base temperature. This is illustrated in Figure 3.6. The mean temperature this day is 13.4°C, which means this is a heating day. At 00:00 the temperature is 12°C with a base of 18 °C. This adds 6 HDD degree hours. At 01:00 7 degree hours are recorded. Between 13:00 and 18:00 the temperature exceeds the base value, so these don't contribute to the HDD. This day a total of 199 degree hours and 19 heating hours are recorded. This is done for the entire heating season to find the total accumulated temperature difference and amount of heating hours.

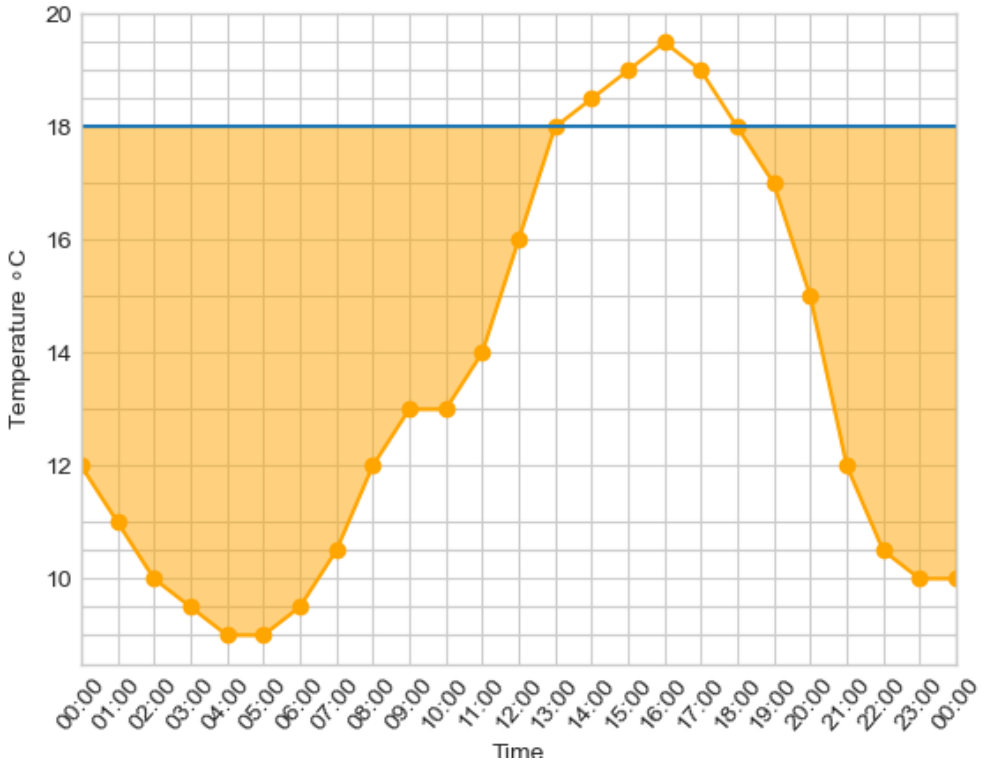

Figure 3.6: Heating Degree Days visualised with a base temperature of 18°C.

The accumulated temperature differences vary each year, but in the Netherlands, it is around 3200 degree hours. The annual amount of heat energy required by a building can be calculated by combining all sources of heat loss.

$$Q_{tot} = Q_{trans} + Q_{inf+vent} - Q_{sol} - Q_{int} \tag{3.15}$$

Where the heat transfer by transmission and ventilation can be calculated using the thermal conductance and the HDD.

$$Q = U \cdot HDD \tag{3.16}$$

Here Q is the heat load of the specific mode in kWh/y, U the heat transfer coefficient of that mode in W/K and HDD the total degree hours per year in KH/y. The heat load by transmission, infiltration, and ventilation can then be calculated using Equation 3.17

$$\begin{aligned} U_{tr} &= \frac{1}{R_{conv} + R_e + R_{conv}} + \alpha \cdot \frac{1}{R_{conv} + R_{floorinsul}} \\ U_{inf+vent} &= c_{air} \cdot (ACH_{inf} + ACH_{vent} \cdot (1 - \beta)) \cdot V_{building} \end{aligned} \tag{3.17}$$

Where α is an adjustment factor for soil that is set at 0.5 in the Netherlands.

The effect of internal generation can be calculated using the total heating hours. This is because internal generation does not reduce the annual space heating requirements if it occurs during times when heating is not required. This also holds true for solar radiation. In Equation 3.18 it is illustrated how internal generation is taken into account. Since ϕ_{int} is time-invariant a simple multiplication holds. Solar radiation however has a strong time dependency. Therefore simple multiplication does not hold and an annual integration is required. This was done using a meteorological dataset that was constructed from hourly averages of measurements of 46 weather stations between 1991 and 2017 [1]. Since the dataset was measured in hours t in Equation 3.19 is the hour of the year.

$$Q_{int} = \phi_{int} \cdot A_{ref} \cdot Hh \tag{3.18}$$

$$Q_{sol} = \sum_{t=0}^{8760} \dot{Q}_{solar}[T(t) \leq 18] \tag{3.19}$$

Chapter 4

Heat pump models

4.1 Working principles of heat pumps

Heat pumps work by extracting energy from a medium and pumping it to heat another medium. Under normal conditions, heat can only flow from hot to cold, by adding energy a heat pump can make heat flow in the other direction. Because heat is extracted from another medium this method of heating is far more efficient than conventional heating while obeying the laws of thermodynamics.

The basis for a heat pump is the ideal gas law which relates the pressure P, volume V absolute temperature T, and amount of particles n with each other for an ideal gas 4.1. Here an ideal gas is a theoretical gas where atoms take up no space and there are no forces present except when collisions occur. In reality, gasses will behave non-ideal and this results in lower than theoretical efficiency.

$$PV = nRT \tag{4.1}$$

In Figure 4.1a a schematic representation is drawn where the thermodynamic cycle it corresponds to is illustrated in Figure 4.1b. This vapor compression cycle is the most common method used to raise low-grade heat to a level where it can provide use full heating. The cycle starts in the outdoor unit where the cold liquid working refrigerant expands after the expansion valve. This decreases the pressure and increases the volume making the fluid a partial gas vapor. Because the refrigerant has a boiling temperature that is lower than the temperature of the cold medium the vapor starts boiling in the evaporator at a constant pressure. This phase change stores latent heat in the refrigerant and raises the temperature according to 4.1. Then the compressor, which is the only part of the system that consumes energy compresses the vapor which decreases its volume and increases its pressure. This greatly increases its temperature

Since the pressure ratio that the pump of the heat pump delivers can be altered, the temperature of the working fluid can be altered at both the cold evaporator side and the hot condenser side. This is advantageous because as seen in the Table A.1 the temperature range for which the buffer vessel operates can be as high as 10-15 °C. Heat always needs a temperature gradient to flow therefore the condenser temperature is set to be 5 °C above the temperature of the vessel temperature. Being able to change the compression ratio and temperatures of the working fluid saves energy because it can be set to be 5 °C above the current vessel temperature instead of the maximum vessel temperature. This is in line with assumptions and findings from [10]. This also holds for the evaporator side. However in this case there needs not to be a temperature gradient since the boiling of a fluid occurs at a constant temperature. Being able to control the evaporation temperature by changing the pressure of the fluid in an Air Source Heat Pump (ASHP) because the temperature of the working fluid can be matched with the outdoor temperature thus a better Coefficient of Performance (CoP) performance can be obtained.

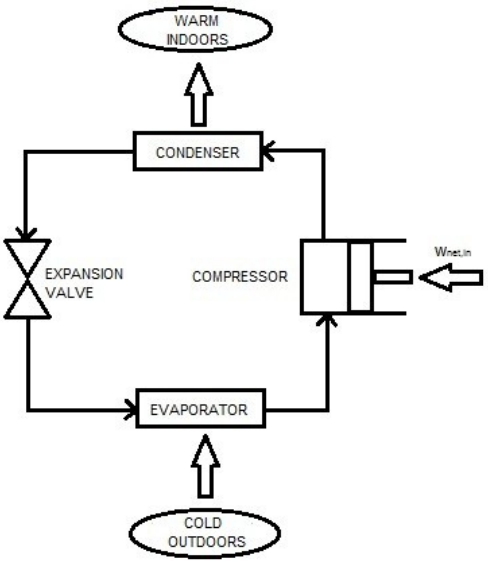

(a) Schematic drawing of the most important elements of a heat pump.

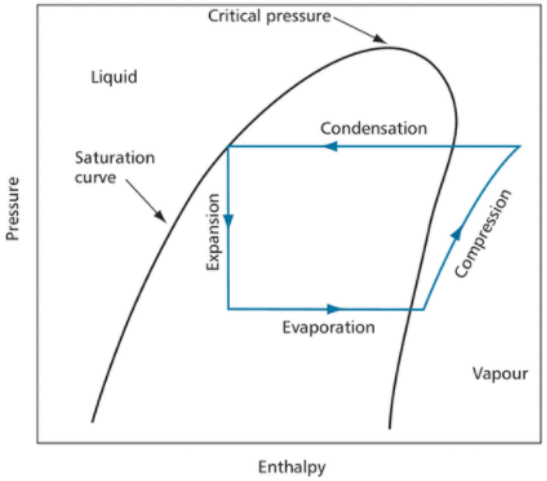

(b) Thermodynamic cycle of a heat pump with saturation curve. Enthalpy is defined as $U + PV$ where U is the amount of internal energy.

A compressor is required to drive the circulation of fluid and provide pressure. A compressor is a mechanical motor that spins and has a certain mass. Every time it starts up it is required to deliver high torque to start the mass which degrades the compressor and its components over time. If this happens more frequently this degrades the system quicker. It is therefore advantageous for the lifetime of the system to have longer cycle times. This however produces more heat in each cycle and because people don't like extreme heat swings in their homes a thermal mass is required to temporarily store this heat. Various ways of doing this will be explained in the next section.

4.1.1 Types of heat pumps

Heat pumps can differ in many dimensions. Figure 4.2 illustrates all relevant technical differentiation's. Below the dotted line are all the variations and aspects that are taken into account for this analysis. The type of heat source and sink is important in characterizing a domestic heat pump system. The type of source and sink greatly affect the efficiency of a heat pump because the temperature difference between them determines the efficiency of a heat pump. Seasonal fluctuation of temperature differences between air is much higher than that of soil or water, leading to lower efficiencies during colder periods. Furthermore, when a heat pump extracts heat from the cold medium it cools that down. When air is used as a heat source this can lead to the freezing of the outside unit, and extra energy is needed for defrosting [14]. The heat sink is linked to the type of heat storage and distribution system. Water is used for radiator and underfloor heating while air is used for heat recovery and ventilation.

When water is used as a heat distribution system this offers the possibility to store heat in buffer tanks and the building structure. Since water has a relatively high volumetric heat capacity (around 750 times greater than air) a lot of thermal energy can be stored this way. This is advantageous for a heat pump since this reduces the number of cycle times of a heat pump.

The type of heat storage also affects how the system will behave. The most common storage methods are the building thermal mass and a buffer tank. In some newer buildings, experiments are done with phase-changing materials which can store large amounts of latent heat. For some larger buildings such as the Eindhoven University of Technology campus boreholes are sometimes used to store heat. In this research, only houses are taken into account, for which a borehole is not a financially viable option. It is assumed that all heat pump systems have a small water buffer tank with underfloor heating as their heat distribution system. When the building is used as

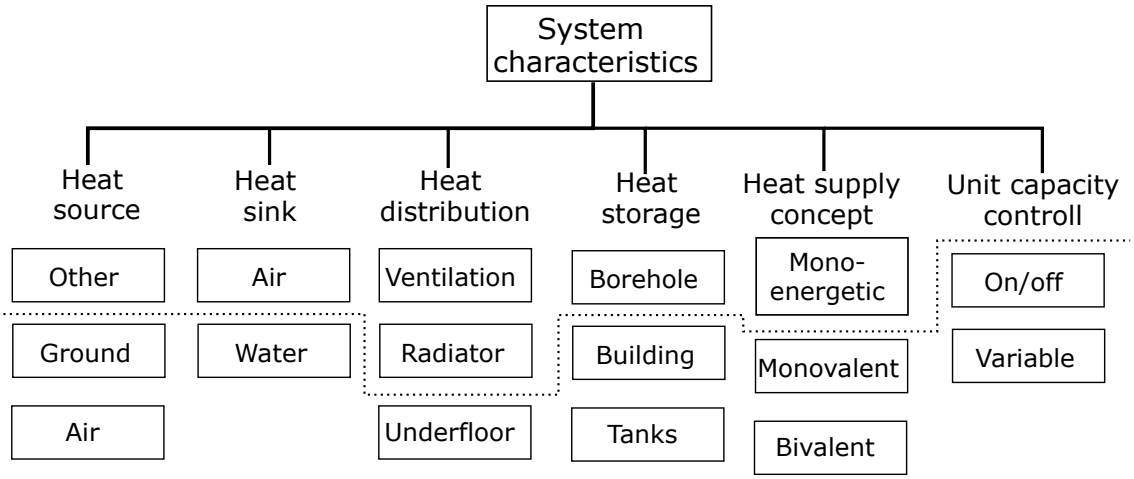

Figure 4.2: Main differential features of residential heat pump systems. Below the dotted has been implemented in this research. Figure adapted from [14]

thermal energy storage this would change the temperature of the internal structure thus affecting thermal comfort. In this research, the underfloor heating system is modeled as having a constant flow rate and the temperature of the supply water regulates the indoor temperature. Therefore part of the building contributes a small part to heat storage as well. In Europe, most of the heat pump systems are connected to a hydronic system and a thermal energy storage tank [14].

Depending on the type of heating system, an additional source of heat can be used to provide support for the heat pump. If all the thermal space demand is met by the heat pump it is referred to as a monovalent system. In addition, an additional heat source may be used for support on colder days. This can be an electric heater (mono-energetic system) or a fossil fuel-based boiler (bivalent). A bivalent system is more commonly referred to as a Hybrid Heat Pump (HHP).

The way unit capacity is controlled is also of importance. Fixed speed heat pumps are operated in an on/off manner whereas variable speed heat pumps allow for a variable regulation of compressor speed in a wide range of operating strategies. This provides better control over large parts of the operation range of a heat pump. This way a better match can be made between the thermal demand and electricity consumption. Research by [27] shows that variable speed heat pumps can but do not necessarily increase efficiency. However, for implementation in a smart grid, they offer a higher degree of operational flexibility and load shifting capabilities [14]. Furthermore, they can have longer cycle times because they can reduce their thermal output, which may be advantageous for the lifetime of the system. A comprehensive analysis between various operating strategies is done in section 4.4 and validated in chapter 5

4.2 Coefficient of Performance

As explained in section 4.1 heat pumps can have efficiencies of more than 100%. The ratio between thermal energy provided and electrical energy required is called the Coefficient of Performance (CoP). In 1824 french physicist Sadi Carnot proposed the Carnot efficiency which is the maximum possible efficiency that a heat pump or, engine operating between 2 temperatures may have. This efficiency assumes perfect conditions with a perfect refrigerant and does not take friction losses or power consumption of other components of the heat pump. A more accurate relationship between CoP was found by [35]. In their paper, they introduced the when2heat dataset introduced which includes hourly measurements of heat pumps from 16 European countries from the years 2008 to 2018. This dataset differentiated between ASHPs and Ground source Heat Pumps (GSHPs). The CoP relations where found by quadratic regression which resulted in Equation 4.2

$$COP = \begin{cases} \frac{T_h}{T_h - T_c}, Carnot \\ 6.08 - 0.09\Delta T + 0.0005\dot{\Delta}T^2, ASHP \\ 10.29 - 0.21\Delta T + 0.0012\dot{\Delta}T^2, GSHP \end{cases} \tag{4.2}$$

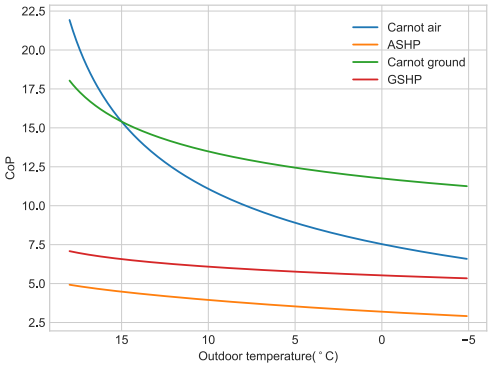

Figure 4.3: Caption

In Equation 4.2 the formulas that where found by [35] are plotted with the hot temperature found by the heating curve + 5°C as described by formula 4.3. For the soil temperature, a constant of 15 degrees was taken. Even though the Carnot efficiency will never be achieved this graph shows that there is still room for improvement for systems that will be installed in the future. For the remainder of this report however, the experimentally found formulas will be used.

Underfloor heating requires lower temperatures as compared to radiators between 35 and 45 °C as compared to 60 °C for radiators [7]. This is because an underfloor heating system has a higher surface area which allows to transfer the same amount of heat with lower temperatures. This can be deduced from Equation 3.9. This means the heating curve is shifted up if radiator heating is applied.

4.3 Tap water heating

Since tap water is a separate system from the space heating system for hygienic reasons there could be three possibilities for heating tap water for this system Figure 2.1.

First, the tap water could be at the same temperature as the space heating water and therefore a heat exchanger could transfer heat from the space heating storage tank to the tap water storage tank. All energy would therefore come from the heat pump unit. A disadvantage however is that tap water is required to be stored at a higher temperature than space heating water, especially if underfloor heating is installed. According to NEN 1006, all tap water in the Netherlands is required to be stored at a temperature of at least 60 °C to prevent and kill legionella bacteria. The efficiency of a Heat Pump (HP) decreases with temperature difference thus this setup will result in an inefficient system. In practice, this system is therefore not applied.

A second method would be to heat tap water with electric resistance heating to the desired storage temperature. This can be seen in Figure 2.1 in case the heat exchanger is not present. Thirdly cold tap water could be heated by the heat pump through a heat exchanger to a temperature of 30 to 40 °C and then boosted to the desired temperature with electric resistance heating. This method is the most energy-efficient and was modeled by [10]. For this reason, this has been applied in this model as well. Furthermore, the design decision was made to prioritize tap water heating over space heating if it was required because the building has thermal inertia and one does not want to shower with cold water.

Regulating the DHW storage tank temperature was done by means of an on/off control at a temperature of 65 °C with a temperature hysteresis of 5 degrees.

4.4 Control strategies

Both a ASHP and a GSHP can be controlled with variable output or have an on/off control. An ASHP is controlled with a variable speed motor on the compressor. A higher flow rate of working fluid will extract more heat from the outdoor air and deposit this in the storage tank. Because more heat is extracted more air is required from which heat can be extracted at the same time. Therefore the fan speed on the outdoor unit is also increased to accommodate a higher airspeed. In a GSHP system with variable power output, the control works similarly but the variable speed fan is replaced with a variable speed compressor on the soil fluid loops.

Since the thermal demand of a building is strongly dependent on the outdoor temperature a building can be heated with much lower temperatures in its heat distribution system when the outdoor temperatures are higher. Therefore the storage tank temperatures can be lower as well which increases the systems' efficiency. The relation between the storage tank temperature and the outdoor temperature is called the heating curve for which various types of formulas have been developed but in reality, the homeowner can adjust the heating curve slope and offset to personal preferences and building properties [11].

[28] thoroughly describes the various control strategies for on/off heat pumps. In essence, they all compare the current temperature of the buffer tank with the heating curve and then decide whether to heat or not. They define the Equation 4.3 to calculate the required storage tank temperature for a given outdoor temperature.

$$T_{s,req} = \frac{\beta \cdot (T_i - T_a) + K_2 \cdot T_i \cdot (\beta - 1)}{K_2 \cdot (\beta - 1)} \tag{4.3}$$

Here T_i and T_{amb} are the indoor thermostat setpoint temperature and outdoor temperature in °C respectively. α and β are auxiliary variables that facilitate calculations of the required storage tank temperature according to 4.4. And K_1 and K_2 are constants that are calculated at the lowest normally expected temperature in the area where the heat pump is installed.

$$\alpha = K_2 \cdot \exp\left(\frac{\ln(K_1 \cdot (T_i - T_a)/K_2)}{1+n}\right) \qquad \beta = \exp\left(\frac{T_i - Ta}{\alpha}\right) \tag{4.4}$$

$$K_1 = \left|\frac{((T_s - T_r)/\ln((T_s - T_i)/T_r - T_i))^{1+n}}{T_s - T_r}\right|_{DOT} \qquad K_2 = \left|\frac{T_i - T_a}{T_s - T_r}\right|_{DOT} \tag{4.5}$$

Here n is the radiator exponent which is a variable between 1 and 2 which is a characteristic of a heat distribution system. T_s, T_r are the supply and return temperatures in °C calculated at DOT. DOT is the lowest normally expected temperature in the area where the heat pump is installed, which is -14 for the Netherlands A.1. A maximum supply temperature of 50 degrees is assumed here with a maximum ΔT of 10°C, which sets the DOT return temperature at 40°C. For radiator exponents between 1 and 2, the corresponding heating curves are shown in Figure 4.4 for an indoor temperature of 20°C. Since the heating curve can be adjusted by user inputs a range between 30 and 40 °C was used in some control strategies.

For on/off type heat pumps there are three methods of controlling when it turns on. "Constant hysteresis", "Floating hysteresis" and "Degree-Minute" method [28]. For a variable speed system, a multiple hysteresis or variant of PID control is applied.

4.4.1 (Floating) hysteresis

In this method, which is sometimes also called bang-bang control, the temperature of the storage tank is controlled by setting the desired setpoint and around which bandwidth is defined, called the hysteresis. The heat pump will turn on if the storage tank temperature drops below the setpoint temperature minus half the hysteresis value, and will remain on until the temperature reaches the setpoint plus half the hysteresis value. This means that if a hysteresis of 5 °C is chosen

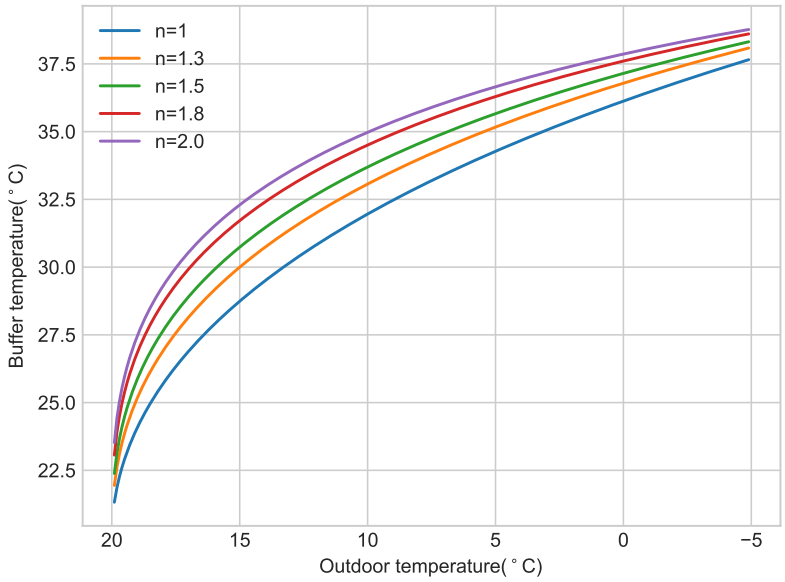

Figure 4.4: Heating curve according to Equation 4.3 with various radiator exponents.

the storage tank temperature is allowed to swing 2.5 °C above or below the setpoint temperature before the heat pump starts or stops [28].

The hysteresis can also be floating. In this method, the hysteresis is changed based on the heat pump status (turning on or off). When the heat pump is turned on or off, the hysteresis increases to avoid too fast a reaction of the heat pump. When the heat pump stays on or off the hysteresis will gradually decrease. This ensures that if switching happens too often, the hysteresis is increased more than it is decreased thus lowering switching. Similarly for too slow switching, the situation is reversed.

$$T \begin{cases} \leq T_{set} - \frac{h}{2} & P = P_{max}, \\ \geq T_{set} + \frac{h}{2} & P = 0 \end{cases}$$

$$Hysteresis_{floating} = \frac{(hysteresis_{max} - hysteresis_{min})}{(t_h/timefactor) + 1} + hysteresis_{min} \tag{4.6}$$

4.4.2 Degree minute method

This method is not implemented in this study because it requires a mono-energetic heat pump system. In this method, the difference between the actual and required storage tank temperature is added each minute to the parameter called the 'degree minute'. The value of this parameter is used to control the heat pump and the auxiliary heater. The heat pump turns on when the degree minute drops below a certain value. If the degree minute value decreases even more at a certain point the first stage of the auxiliary heater turns on. If the value decreases further progressively the auxiliary heater turns to higher power bands. This increases the temperature of the buffer tank. If the temperature increases above the setpoint temperature the degree minute value increase again. As it increases progressively more the auxiliary heaters turn off and eventually it reaches 0 and the heat pump turns off too. This method can be seen as a Proportional Integral (PI) controller with discrete power band 4.4.4.

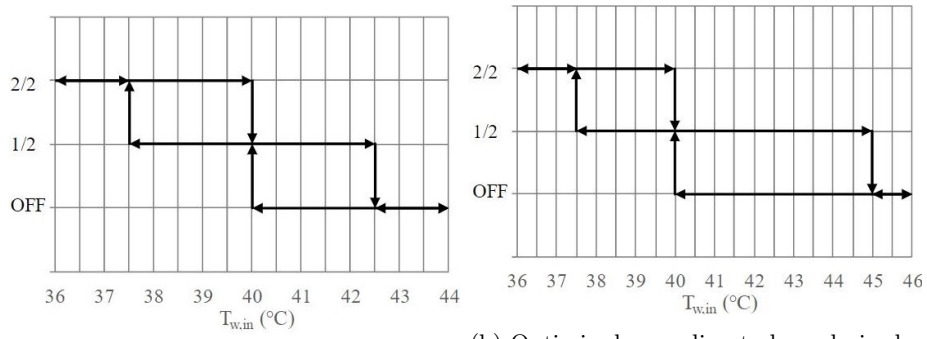

(a) Balanced

(b) Optimised according to boundaries by [13].

Figure 4.5: Variants of 2 stage hysteresis control as proposed by [13].

4.4.3 Multiple hysteresis

Multiple hysteresis control of a heat pump can be used in a situation where the power input of a heat pump is not continuously variable but has discrete power bands. [13] modeled the working of 2 stage heat pump versus an on/off the type heat pump and optimized for the first switch and upper bound temperature for a certain building typology. The original control logic and optimised logic can be seen in Figure 4.5a and Figure 4.5b. The building they modeled used radiators for heat distribution and an additional thermal storage of 11.2 l/kW to limit the frequency of on-off cycles. The radiators had a design supply temperature of 45 °C.

The operating strategy is quite simple and only depends on the current temperature of the storage tank. With the original parameters, it can be seen in Figure 4.5a that if the water temperature is above 42.5 °C the heat pump shuts off completely. As the water cools the heat pump remains off until it reaches 40 °C at which point the heat pump turns to half capacity. This heats the storage tank. However if the heat demand is higher than the output of the heat pump it will cool down more, and at some point, the lower temperature band is reached. This triggers the second stage of the heat pump to turn on which will be turned on until 40 °C is reached at which point the second stage is turned off. As can be seen in Figure 4.5a the current power output of the heat pump is not only dependent on the instantaneous value of the storage tank temperature but also on the direction the temperature is changing. After optimisation for energy consumption with a penalty for switching constraints the values of Figure 4.5b where found by [13].

4.4.4 PID control

A Proportional Integral Derivative (PID) is a type of control loop mechanism that applies a feedback loop from an operation sensor to correct for the input signal. It is only suited for a Variable Speed Heat Pump (VSHP) since it provides a continuous output signal. It is widely used in industrial control systems and is by far the most common feedback control mechanism for industrial processes. It has been estimated that over 95% of industrial control loops that require continuous feedback control are some variation of a PID controller. The working of a PID control loop is fairly straightforward. The current setpoint of a process is compared with the current output value of the process. This is called the error e of the process. This error is split over 3 different paths. In the proportional path, the error is multiplied by constant K_p, in the integral path the error is integrated and multiplied by constant K_i, and in the differential path the error is differentiated and multiplied by constant K_d. All the error terms are summed and will result in an output signal. The output signal is the input to the heat pump and it will respond accordingly. The result is measured and fed back to the controller for continuous readjusting. Figure 4.6 depicts this schematically.

The general formula for a PID control function is:

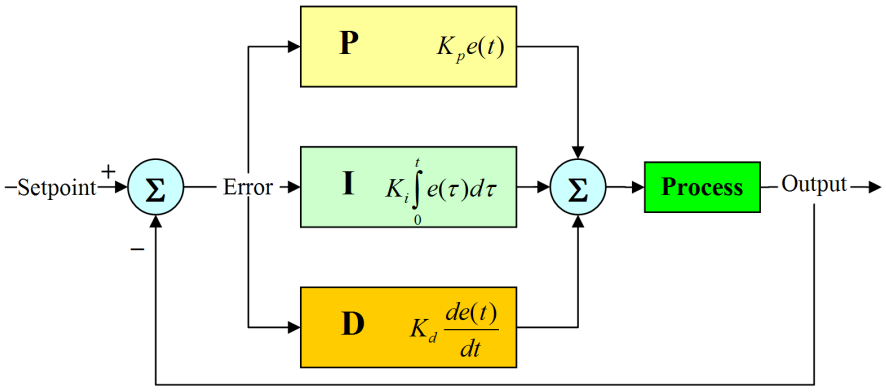

Figure 4.6: Schematic drawing of the working of a PID control loop.

$$u(t) = K_{\mathrm{p}} e(t) + K_{\mathrm{i}} \int_0^t e(\tau)\,\mathrm{d}\tau + K_{\mathrm{d}} \frac{\mathrm{d}e(t)}{\mathrm{d}t} \tag{4.7}$$

where K_{p}, K_{i}, and K_{d}, all non-negative and denote the coefficients for the proportional, integral and differential terms (P, I and D) respectively. Either or either combination of gains can be set to 0 to exclude it from the controller (e.g. $K_{\mathrm{d}} = 0$ becomes a PI controller, and P controller with K_{i} and $K_{\mathrm{d}} = 0$). In case of a VSHP that will heat a buffer tank to T_{set} the control in the various controllers will be:

P-controller In this case the output power of the VSHP is only dependent on the difference between the current temperature and the setpoint temperature. As the buffer tank temperature approaches the setpoint temperature the power output will also decrease. It is the simplest form of control which makes it the easiest to tune. It provides a rapid kick response to both setpoint changes and disturbances. This makes it the most robust (i.e. stable) type of control, but it is susceptible to offset. If properly tuned this would be enough for the tank to reach the correct temperature.

PI-controller In this case the integral gain also contributes, this can eliminate constant error from the system. If for example, someone is taking a bath, there will be a constant draw-off rate for a while, so the P-controller would keep the buffer tank at a constant steady-state that is below the setpoint temperature. The integral error however will add up and make the VSHP increase its power output to eliminate this error. For the application of buffer storage tank and water heating, it is debatable if it is necessary to include integral gain. The ability to remove steady-state error makes this the most common configuration of the PID control.

PID-controller Combines all three terms. The derivative term allows this type of control to react much quicker to a change in environments and will result in more stability and a decrease in the overshoot of the desired value. However, when the sample time is low and the input signal is noisy it can quickly destabilize the loop. Even small variations, when divided by a very short timestep result in big differences in the output signal.

P and PI controllers are the most common controllers in VSHPs [10]. The instability that the differential of control loops component can cause is the main reason. An unstable control loop will cause excessive component wear since accelerating and decelerating compressor fans puts higher torque loads on components. Since it poses no direct benefits for simple applications such as buffer tank storage temperature regulation only the P and PI controller were simulated.

To prevent excessive component wear modeling a VSHP was combined with a temperature hysteresis where the setpoint was switched between the upper and lower temperature bands.

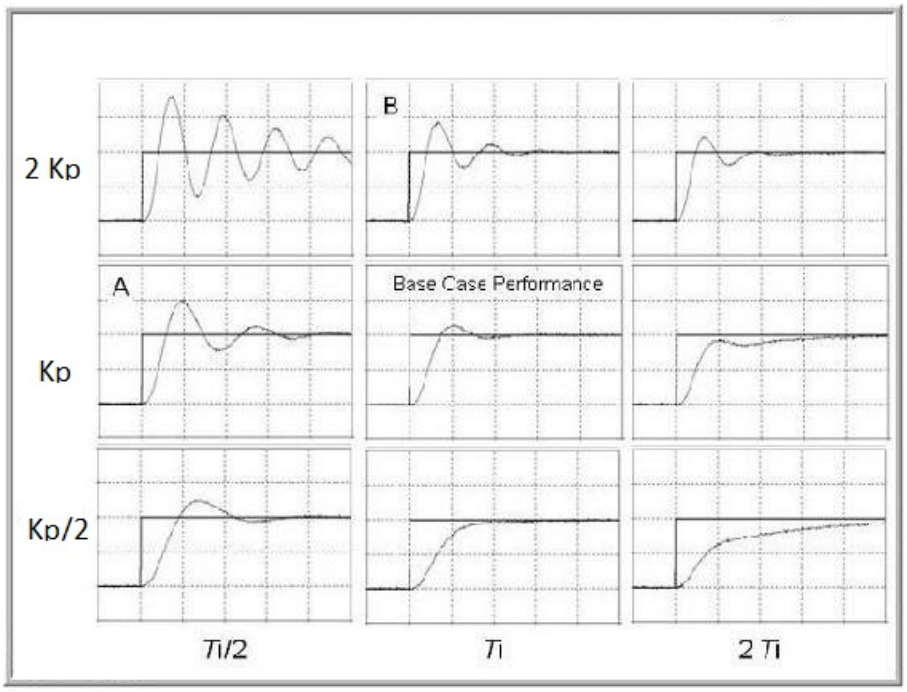

Figure 4.7: Impact of Kp and T_i on performance of PI controller of the form 4.7

4.5 Tuning PID control

Tuning a PID controller is finding the values of proportional, integral, and differential gains so the system behaves in a certain way and meets certain design requirements. It depends on the characteristics of the situation and the system. Therefore a one size fits all tuning method doesn't exist and final prescribed values don't exist in the literature, but studies have been done to find values that achieve a certain goal. For example [23] investigated the influence of various PI parameters of underfloor heating controllers on energy consumption. [22] investigated optimal PI parameters for accurate temperature control in underfloor heating. [13] used a PI controller to modulate an inverter drive heat pump where the PI parameters have been chosen according to manufacturer data where the values of K_i ad T_i have been set to 10 and 300 s.

in Equation 4.7 K_i and K_d can be written in terms of K_p by introducing the terms T_i and T_d. K_i and K_d then become K_p/T_i and K_pT_d respectively.

the advantage of this is that T_i and T_d have some understandable physical meaning, as they represent an integration time and a derivative time respectively. K_pT_d is the time constant with which the controller will attempt to approach the set point. T_i/K_p determines how long the controller will tolerate the error being consistently above or below the set point.

4.5.1 Tuning PID control for underfloor heating

In section 4.5 was described how a form of PID control can be tuned. The integral gain was expressed in form of a time constant and integral gain. This section will explain how the underfloor heating controller is tuned for a general model.

Since the building dimensions are variable for different simulations one of the following strategies must be applied.

- Tuning Kp and Td before every simulation with an automated algorithm
- Tuning once and using the same parameters for every simulation.

It is therefore important to find a relationship between floor area and tuning parameters since every building in the simulation should have a stable floor heating control loop. In reality, if people find that their heating system is constantly overshooting and undershooting the thermostat set point temperature they consider it broken and will have someone fix it. Fortunately, we can begin by stating the formula of the thermal time constant, which is defined as the time it takes for a system undergoing heating or cooling to reach 63.21% of the initial temperature gradient. In mathematical form, this results in the following equation.

$$\tau_{th} = \frac{\rho V C}{h A_s} \tag{4.8}$$

where τ is the thermal time constant, ρ the density of the material, C the heat capacity of the material, h the heat transfer coefficient of air, and A_s. Since the thickness of the concrete in underfloor heating is modeled as a constant in the model the thermal time constant becomes independent of the floor area. Using the parameters from Table A.1 the time constant becomes approximately 21.120 seconds (352 minutes).n

Tuning a PI controller does not only depend on physical properties but also on preferences and demands for various types of responses. For example demands on maximum overshoot, the rise time, settling time, and tolerable steady-state error (and duration). It does however show that independent of surface area the thermal system will react the same. For slow reacting systems a high gain and low integral time constant should be used. Various studies have been performed to study optimal PI parameters and their influence on energy efficiency and comfort [22, 23]. Here values of $K_\mathrm{p} = 10.000$ and $T_\mathrm{i} = 10.000s$ have been used.

These values were found by various adjustments of Kp and Ti to come to the desired value. A more systematic approach would be for example Siegler-Nichols or Cohen-Coon. These however only provide good first guess indications and no definitive answers, since tuning depends on preferences and system desires.

In Figure 4.8 9 variations $K_\mathrm{p} = 10.000$ and $T_\mathrm{i} = 10.000s$ and their corresponding temperature response have been plotted for a 24 hour period. Here it can be seen that decreasing Kp to about 5.000 will result in significantly slower response and overshoot of the desired variable. Increasing Kp will result in a faster response but is also demanding on the system because when their power curves were investigated they quickly approached the maximum power output that was deliverable by the heating system. Decreasing Ti to 50% of its original value would result in a higher overshoot while decreasing it would compromise on settling time.

In Figure 4.9 the corresponding temperatures and power response of the room and underfloor heating system have been plotted.

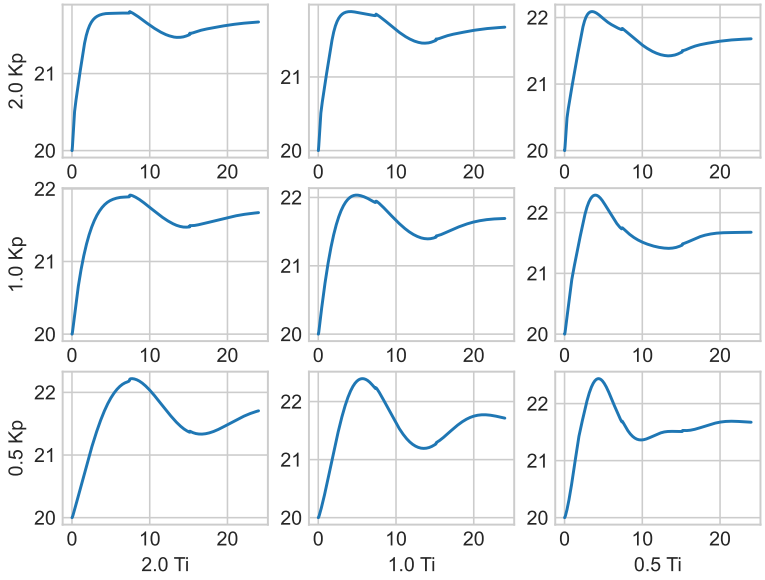

Figure 4.8: Effects of varying Kp and Ti on settling time for the floor temperature. A base of $K_{\mathrm{p}} = 10.000$ and $T_{\mathrm{i}} = 10.000s$ have been used.

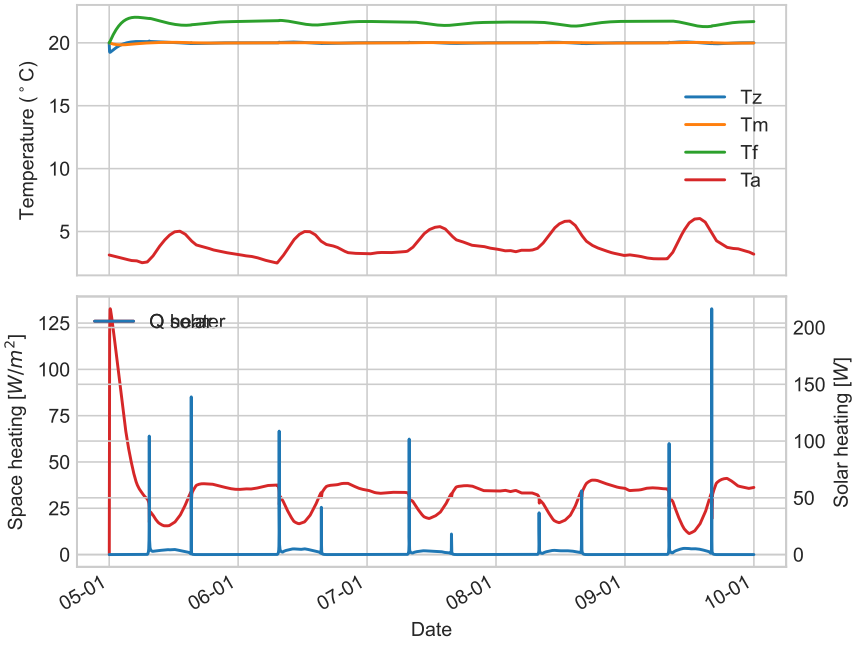

Figure 4.9: Response of power and indoor temperatures on a tuned underfloor heating controller where the red line on the bottom figure is the power output of the underfloor heating system. As the outdoor temperature fluctuates the power output of the controller responds accordingly minimizing the temperature fluctuation in the room. Tz: zonal temperature, Tm: temperature of the internal structure, Tf: temperature of the floor, Ta: ambient temperature

4.6 Hybrid heat pumps

Hybrid Heat Pump (HHP) combine a HP with a gas-fired boiler to provide heating. It can switch between energy sources depending on specified conditions. This has the benefit that the HP unit is not required to be sized to accommodate the coldest day because an alternative heating method is available. This means the heat pump unit can be much smaller than if a full electric heat pump is installed. Although the general definition of a HHP permits any other fuel as the alternative heat source, we will limit our definition to a HHP to a ASHP combined with a gas-fired boiler and a controller.

This is especially attractive for retrofitted houses since their insulation standards are lower, therefore, requiring higher heat distribution system water temperatures for heating the building. Heat pumps are not efficient at those higher temperatures. HHPs can be configured such that the ASHP preheats the water to a certain temperature (for example 40 °C) and then the gas-fired boiler boosts the temperature to a point that is sufficient to heat the building for the current outdoor temperature. Also, the DHW can be heated using the gas-fired boiler which boosts the efficiency of the ASHP. Furthermore, the installation of a HHP system is much cheaper than a full electric heat pump [15]. The main reason is that a much smaller heat pump unit can be installed since it does not have to be designed for the coldest temperature.

To gain insight in performance of actual HHPs the Dutch project installatiemonitor was launched [18]. The goal was to gain insight into the consumption of natural gas in HHPs as well as to calculate the seasonal CoP. A combination of smart meter data and interview questionnaires was combined to identify consumption patterns. A set of 450 HHPs was deemed of high enough quality for further analysis. They found that about 60% of the annual thermal demand is met by the heat pump unit, and the other part is met by the gas-fired boiler [18]. Their findings per temperature can be seen in Figure 4.10. Modeling of the HHP was done by using the share of thermal demand that was met by the gas-fired boiler per temperature according to 4.10 in combination with a ASHP. Here it is assumed that the heat pump uses the same control strategy as a full electric ASHP with the corresponding output. The gas-fired boiler adds extra thermal energy according to Figure 4.10. For example, if the outside temperature is 2.5 °C and the heat pump generates 2 kW of thermal energy, the gas-fired boiler provides an additional 2 kW of thermal energy.

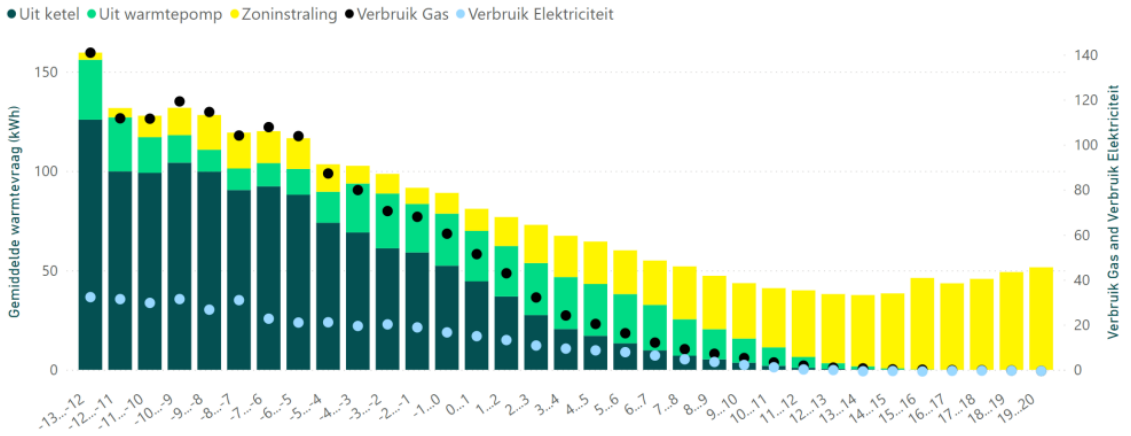

Figure 4.10: Space heat demand of buildings met by various sources in a hybrid heat pump. Dark green: natural gas, light green: heat pump, yellow: solar radiation. Black dots: gas usage, blue dots: electricity consumption. At extremely low temperatures the heat output of the heat pump seems to increase. This is a statistical fluctuation in measurements due to the very limited amount of measurements available at these temperatures and will for this research be regarded as zero. Measurements done by [18]

4.7 Sizing of heat pump and buffer tank

In the Netherlands, the natural gas is built to accommodate outdoor temperatures of -14°C. It could therefore be assumed that heat pumps installed in buildings should be able to withstand these temperatures as well. However: heat pumps are expensive devices to install. Installation of a full electric ASHP range from €4000 to €7000 including installation excluding subsidies [3]. For a GSHP this ranges from €10000 to €25000. For an ASHP the unit costs comprise around 60% of the total costs of the heat pump. Since these costs increase with higher capacity systems homeowners want to select a system that can provide enough heat during an average winter but are unlikely to greatly over-dimension their system. It is assumed that an expert will advise individual homeowners on the system requirements they should adapt. However a general industry standard is found in Equation 4.9

$$P_{hp} = \frac{Q_{annual}}{FLhours} \qquad (4.9)$$

Table 4.1: FL running hours

Thermal demand W/m^2	FL running hours
100	2854
90	2422
85	2146
80	1878
70	1634
50	1409
45	1201
40	1012
35	961

Where P_{hp} is the electric power of the heat pump, Q_{annual} is the annual thermal space demand, and FL running hours are the running hours of a heat pump at full load. The full load running hours can be found in Table 4.1. Each heat pump that is simulated is connected to a building thermal network, of which the properties are known. The building size and amount of floors determine the total living area. The annual thermal space heating demand can be calculated as explained in section 3.5. With this information, we can read the amount of full load running hours in Table 4.1. With the annual thermal demand and full load running hours, the heat pump power can be computed with Equation 4.9. The industry standard is found at [3]. Furthermore, it is assumed that a HHP uses an ASHP which has a rated power that is 30% smaller than of a full electric ASHP.

4.7.1 Sizing of buffer tank

As explained earlier frequent on and off cycling is bad for a heat pumps' life cycle. Therefore a buffer storage tank functions as a heat sink that allows the heat pump to have longer cycling periods. A higher rated capacity heat pump requires a larger buffer storage tank. ISSO 72 states that a heat pump requires a minimum runtime of 10 minutes at designed conditions. A generally accepted hysteresis of 5 °C as mentions in section 4.4 indicates water is heated for 10 °C. Therefore the following equation can be deduced from the energy balance.

$$\begin{aligned} E_{hp,out} &= E_{buffer,in} \\ P_{el,hp} \cdot CoP_T \cdot t &= c_{water} \cdot \Delta T \cdot V_{buffer} \\ V_{buffer} &= \frac{CoP_T \cdot t}{c_{water} \cdot \Delta T} \end{aligned} \qquad (4.10)$$

Where E is energy in J, $P_{el,hp}$ is the electrical power of a heat pump in Watts, CoP_T is the CoP at minimum buffer design conditions, t is the minimum runtime in seconds c_{water} is the heat capacity of water in $J/(L°C)$, ΔT is twice the hysteresis and V_{buffer} is the volume of the buffer tank in L. For both ASHPs and GSHPs the maximum source temperature is set at 10°C and heat supply temperature is 35°C. This is stated as industry standard by [3] and is in line with

Figure 4.4. Using formulas 4.2 and a hysteresis of 5 °C it can be calculated that an ASHP requires a storage tank of roughly $60 L/kW$ and a GSHP 80 L/kW.

Chapter 5

Validation of synthetic profiles

The theory of how heat pump load profiles were generated has been explained. However, it is important to test theory against reality to verify that the profiles generated are in line with actual load profiles of heat pumps. This will be done by comparing actual load profiles to synthetically generated ones. A visual comparison will indicate how close they match.

Two different datasets were included for comparison. The first was a dataset generated in the project 'Your energy moment'. Measurements of 39 GSHPs were done between 1 October 2013 and 1 March 2014. The project continued after that but an algorithm for flexibility creation based on a differentiable price scheme was introduced. Therefore the measurements after this period are not suitable for comparing load profiles that don't incorporate this behavior. The information recorded for all houses were outside temperature, indoor temperature, and heat pump energy consumption. The corresponding buildings are also known to the author so a close match of physical building properties could be selected. The second dataset included around 700 air and ground source heat pumps that were installed via the renewable heat premium payment scheme of the UK. Data was collected between 31 October 2013 to 31 March 2015. A range of dwelling age classes insulation standards and household compositions was present in the study but these characteristics could not be matched to individual profiles. The temperature was also not recorded. Temperature measurements of the corresponding period were also not publicly available and of high enough quality to be used in the simulation. Therefore it was assumed that in the UK the weather was similar to the Typical Meteorological Year (TMY) of the Netherlands.

The various control algorithms explained in section 4.4 produce a variety of different profiles. Therefore several will be compared to measured data in order to determine suitable control strategies. This will be done on an individual profile level, as well as on an aggregated profile level. When the load profiles of various individual heat pumps were explored they indicated various strategies and large differences between them were found. This indicates that in practice a variety of control strategies are applied by various manufacturers.

Table 5.1: Controllers present in validation

Nr	Controller	P [kW]	Sp	Hyst	Tunings	RT [min]
1	Mult. hyst	2.2	40	-	37.5, 45	20
2	Mult. hyst	2.2	HC*	5	1 degree	20 switch
3	Proportional (P)	2.2	HC	5	10	20
4	PI	2.2	HC	5	10, 300s	20

Table 5.2: Boundaries

Property	Value
Type	SFH
Year	2005
Insulation	Level 2
Dimensions	7x10 m
Buffer capacity	60 L per kW
Type	ASHP

The first controller is the optimised control algorithm proposed by [13] which can be seen in Figure 4.5b. It uses set temperatures to switch between 100%, 50%, and 0% power output. After switching between power bands no minimum run-time requirements. The second controller

is similar to the first but with different power output for every degree. The difference is linearly spaced and since the difference between the lower and upper temperature is 10 °C 4.4.1) each degree °C decrease increases its power level by 10%. This type of control is expected to switch between various power bands much more often therefore a minimum run-time for each power level of 20 minutes is introduced. This also eliminates the 'stair step' energy profile, in which every power level is always tried when increasing or decreasing power. The third controller is aPcontroller with a proportional gain factor of 10. The last controller is a PI controller with the same gain and an integral repeat time of 300 seconds. These values are in line with values found by [10]. ThePand PI controller both had a minimum run time of 20 minutes, but no minimum time between power band switches. The minimum run time was chosen to reduce the cycling degradation of the heat pump. Furthermore, the resolution of measurement data is a 15-minute interval, which makes an analysis of a lower switch time not possible.

The comparison was done on a specific house for which the conditions can be seen in Table 5. The dimensions were chosen because according to the CBS the average living area for SFHs in the Netherlands is 141 m^2 [6]. The simulated building has 2 stories, therefore, having around 140 m^2 of living area.

5.1 Visual comparison

The heat pumps from chapter 5 where simulated using the boundary conditions from Table 5. Three types of simulations were done. First, a single heat pump is compared to a single heat pump from both sets of measured data. Some individual attributes of the controllers can be observed in this manner. The second comparison was done on the average of a set of 30 simulated heat pumps and the average of all measured data. Because of the many factors that can influence individual profiles, it is hard to predict if the individual heat pump behavior of a heat pump results in a correct profile on an aggregated level. The last comparison was done by simulating a nighttime setback temperature. This was done because the measured data in the UK seemed to exhibit this behavior. The nigh time setback was modeled according to a gaussian distribution of the wake-up time, sleep time, daytime temperature, and nighttime temperature. This was done to simulate more realistic human behavior. Furthermore, if this was not done all heat pumps start at the same time in the morning resulting in unrealistic high peak loads at these moments. For all profiles, the first two days of the simulation have been trimmed off to exclude the settling time of indoor conditions.

In Figure 5.1 the behavior of individual heat pumps can be seen. Both from the JEM and the UK dataset a sample was drawn which remains constant for all control strategies. The behavior of the heat pump in the JEM dataset is different from the UK measurement. Heat pumps present in the JEM pilot are single speed GSHP with an electric resistance heater for DHW production. They show a tendency to remain turned on for a long period of time whenever they are turned on. Indoor temperature measurements revealed that within this time an indoor temperature swing of 1.84 °C was recorded, with simulated data this was 0.2 (maximum of all control strategies) °C and for the UK dataset, this data was unavailable. This can partially explain the long cycle time, but not fully. Other possibilities are a high thermal storage capacity or an under dimensioned heat pump.

Both MH1 and MH2 seem to display characteristics of the heat pump found in the UK dataset Figure 5.2. Some of the peaks are displayed in a similar fashion and switching between power outputs is similar. In the measured dataset, however, two distinct activity periods can be distinguished while simulated data activity indicates a more constant activity. This might hint at a nighttime setback temperature for the measured UK dataset. The PI controller seems very aggressively tuned. Sometimes it chooses an intermediate power band but overall it will prefer maximum power output for a shorter duration. The P-controller prefers a very constant power output and only corrects when it is absolutely required.

When profiles are combined as seen in figure 5.2 MH1 displays more twitchy behavior than MH2. This is likely due to fewer power levels to choose from, therefore requiring more profiles to

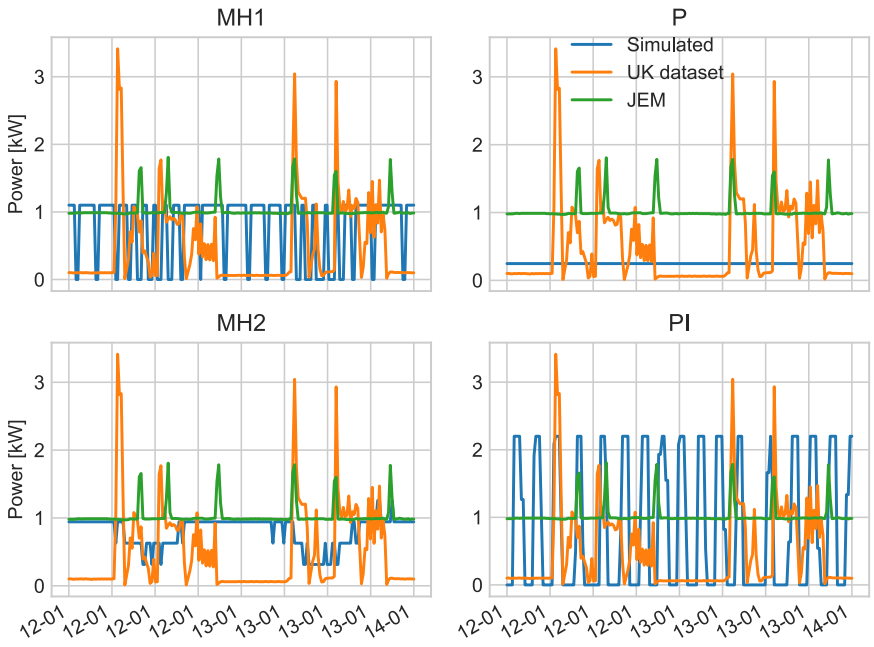

Figure 5.1: Single heat pump comparison for multiple control strategies.

smooth out. MH1 represents the data fairly well while MH2 is too smooth. The small individual peaks in the P-controller are smoothed out. The PI controller displays very twitchy behavior which is larger than the measured data. It is unlikely that many PI controllers were present in the measured dataset.

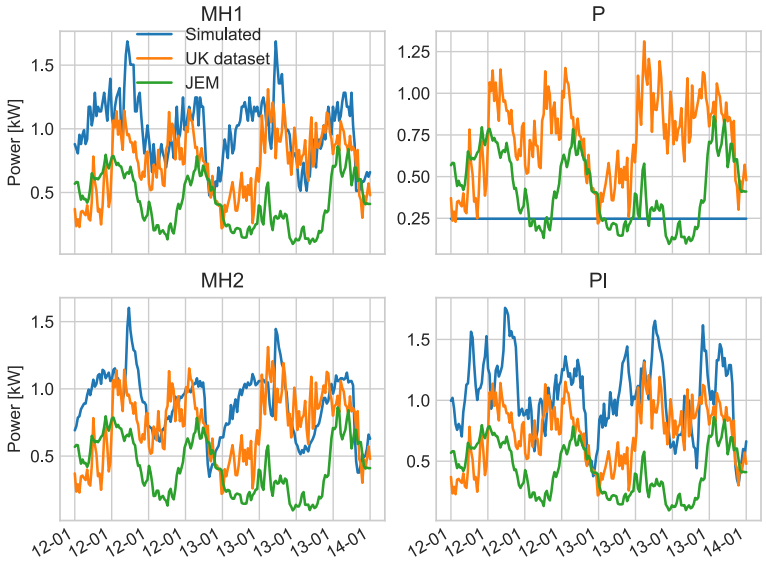

Figure 5.3: Same as Figure 5.2 but with nighttime setback temperatures.

Table 5.3: Setback conditions.

	mean	std
Start	08:00	20 min
Stop	21:00	20 min
T in	20	0.2 °C
T out	19.7	0.2 °C

Nights are generally cooler than daytime periods. This lowers the CoP and increases the temperature difference which increases the heat demand according to Equation 3.11. This effect however was not enough to explain the temperature swings observed in the measured data. When a nighttime setback temperature is included in the measured data the simulated data quite

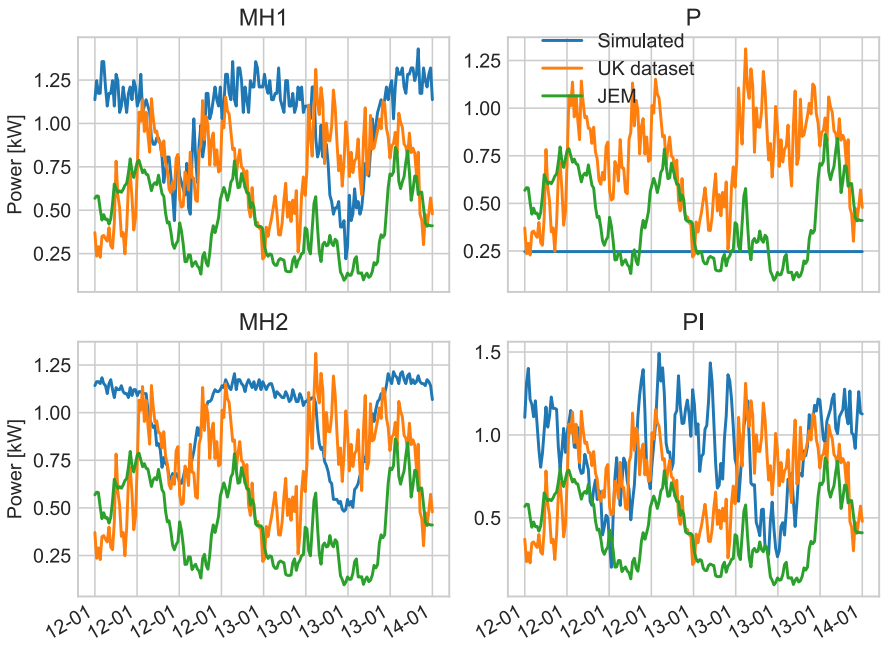

Figure 5.2: Mean of aggregated profiles. 30 synthetically generated, and mean of 30 sample profiles in the datasets.

nicely follows the periods of the measured data. It seems that some homeowners turn down their thermostats slightly during the night. This effect can be observed in both the JEM and the UK datasets. Although it is generally advised against when underfloor heating is used it seems that some homeowners still do this. Therefore the nighttime setback values from Table 5.3 will be used in the simulation for the case study in the next chapter.

Indoor temperature measurements from heat pumps in the JEM dataset were available. Analysis of these temperatures revealed that relatively high-temperature swings were present during the measurement period resulting from the long cycle time of the heat pumps. This revealed that the heat storage strategy of these heat pumps was a combination of building thermal mass and water tank storage Figure 4.2. As mentioned in subsection 4.1.1 this strategy may result in thermal discomfort for dwelling occupants. Additionally, the JEM dataset contained only GSHPs, whereas the UK dataset and the simulated profiles used ASHPs. Since ASHPs are highly affected by outdoor temperatures and GSHPs are not the UK dataset was seen as a more important reference.

When the profiles which included nighttime setbacks were analyzed it seemed that there is no single control strategy that perfectly explained the measured data. MH1 was closest but it started heating a little early on the 13th. MH2 is fairly similar to MH1, but it is less twitchy than the measured data. This is quite obvious since it is the same control strategy but with more power bands to vary between. When compared to the measured data it seemed too smooth. The general form of the PI controller closely matches the data but it seems too spiky. The P controller does not represent the data well at all which might hint at a wrong implementation of this controller. In reality, every manufacturer will program its own controller and thus utilizes its own control strategy. The measured data likely contains more than a single control strategy. If MH2 and PI are combined the smoothness is more similar to the measured data than both of these profiles separate. Therefore the case study in the next chapter will use a homogeneous mix of MH1, MH2, and the PI controller.

Chapter 6

Case study: Den Bosch

To study the impact that heat pumps will have on the electricity grid, a case simulation will be done in 's-Hertogenbosch. This method is applicable everywhere in the Netherlands, but a smaller geographical region is selected to limit the computational overhead and make reporting possible in this paper. A set of 22 transformers are examined under various adoption rates for heat pumps to investigate what the maximum load will be and if it exceeds the current network constraints. For this simulation it is assumed that the weak point in the network is the maximum transformer loading and not individual cables, thus only the medium to low voltage transformers are considered. This is a reasonable assumption since the capacity of all cables that are connected to a transformer combined exceeds the capacity of the transformer. Furthermore, it is assumed that all heat pumps are 3-phase connected and the transformer load is currently balanced. This means that only the maximum total capacity is considered. Measurements during January and February 2021 are taken at a 15-minute interval for 22 transformers in 's-Hertogenbosch.

The general approach for this case study entailed the following steps:

1. Obtain power and gas consumption measurements for the winter period of all transformers in 's-Hertogenbosch
2. Filter data and make distribution fits of gas consumption patterns.
3. Use random variates drawn from the gas consumption of households to determine their annual thermal energy needs.
4. Select representative buildings for the area based on the building classification and adapt input variables so their annual thermal demand is in line with actual annual thermal demand.
5. Sketch scenarios, run the simulation, and add heat pump electricity demand to current transformer loading to answer the main research question.

The buildings that are connected to each transformer are registered in the Enexis database, therefore their annual gas consumption from 2021 could be obtained. More detailed BAG data on the postal-6 code level was not available, therefore an estimation of the building types (based on gas consumption) is explained later in this chapter. To ensure only residential buildings are included in the only gas connections that have physical connections G4 and G6 (capacity of $6m^3/hour$ and 8 $m^3/hour$ respectively) are included in the data since only these are typically installed in residential buildings. Higher capacity ones such as G10, G16 G25, or even bigger are usually reserved for industrial complexes and office buildings. Furthermore, postal codes with annual gas consumption of more than 5000 m^3 were omitted since this consumption quantity is unlikely to be explained by residential building space heating. If it is a residential building it is likely to be explained by swimming pool heating. Furthermore, connections that did not have any gas consumption were omitted. The last omissions were due to specific descriptions in the connection description, such as storage facility, metalworking company, or logistical company. Only company buildings were omitted in this sense. This resulted in the following building omissions:

- No G4 or G6 connection: 47 omissions
- No data available: 2 omissions
- Gas consumption of 0 m^3: 10 omissions. These buildings likely already have a HP
- Gas consumption of > 5000 m^3: 13 omissions
- Building has functional business use: 207 omissions.

Additionally, only transformers that have more than 100 connections after the previously mentioned omissions were taken into account. This resulted in 9 transformers in 's Hertogenbosch that were not included, leaving 13 transformers available for further analysis. This was done for 2 reasons. First, statistical fitting is very prone to errors if few measurements are available. Some estimation of other transformers could have been applied, but since these transformers have so few connections, but a very high rated power it is very unlikely that problems will occur here.

The gas consumption profiles of the houses connected to a transformer are displayed in a histogram in Figure 6.1. The data is normalized and a skewed normal distribution is fitted. Various kinds of skewed distributions were tried such as a lognormal, powerlognormal, Weibull, and chi-square distribution. Then the Kolmogorov-Smirnov test (K-S) test was applied to identify which distribution best explained the data. This led to the result that the skewed normal distribution best explained most of the transformers followed by the chi-square distribution. However, the skewed normal distribution lives in the domain $[-\infty, +\infty]$ whereas the chi-square lives in the domain $[0, \infty]$. Since the gas consumption can never be negative the chi-square distribution was a potential candidate. However, the upper bound in reality is also limited due to piping and availability constraints so it was decided to use the skewed normal distribution since this distribution explained the data best.

To quantify how well the distribution explains the data a non-parametric test (meaning normality is not required) is needed since the data is not normally distributed. In this case, the popular **Kolmogorov–Smirnov test** was used since it can serve as a goodness of fit test. It compares the cumulative distribution function of the distribution with the given data. An example can be seen in Figure 6.2a. Intuitively it takes the largest absolute difference between the 2 distributions across all x values (displayed by the arrow in Figure 6.2a called the D-value. Theoretically, if the distributions are the same, this D-value should be 0. In reality, however, because the samples are drawn randomly from a population this does not hold since even if they are exactly the same due to random sampling. They will differ somewhat. Therefore Kolmogorov calculated the expected distribution of D if the null hypothesis is true. The null hypothesis is that both samples are drawn from the same distribution. The example transformer shown in Figure 6.2b has a D-value of 0.013 and a p-value of 0.657 meaning that the data has a 65.7% chance of being from this distribution.

The gas consumption was grouped by transformer, 9 of which are displayed in Figure 6.3

Grouping gas consummations per transformer and fitting them individually instead of combining all the data and then fitting is more precise. In Figure 6.3 it can be seen that dwellings connected to some transformers are more skewed to lower consumption profiles than others. This is likely due to dwellings that are in urban areas consuming less heat because of their smaller building size. Also in urban areas, there are more Single family home present that don't share facades with neighbors, which increases their loss area.

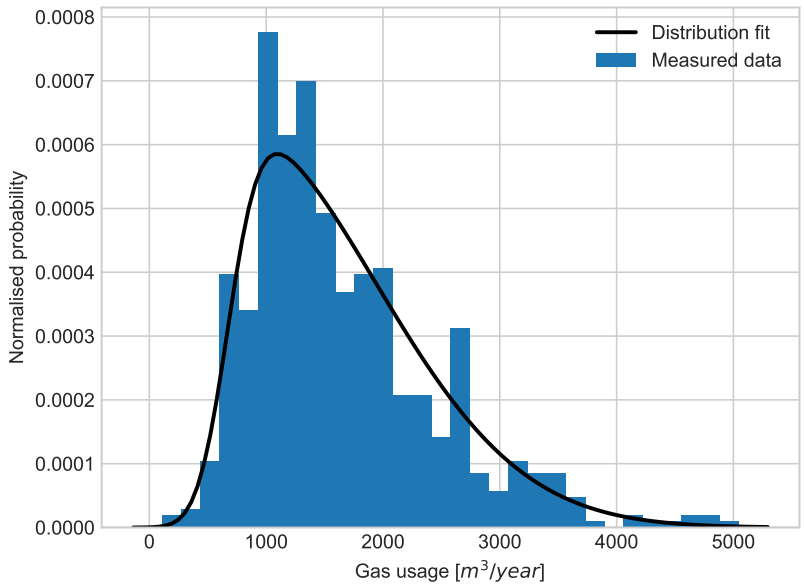

Figure 6.1: Skewed normal distribution fit for the annual gas consumption. Skewness = 6.0, loc = 676, scale = 1260. The distribution is highly positively skewed since gas usage is always positive.

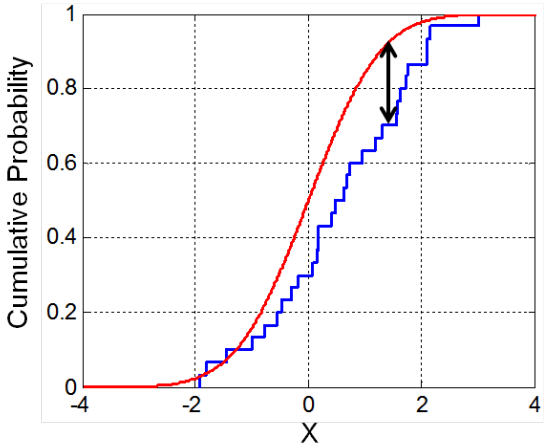

(a) Design schematic of Kolmogorov–Smirnov test.

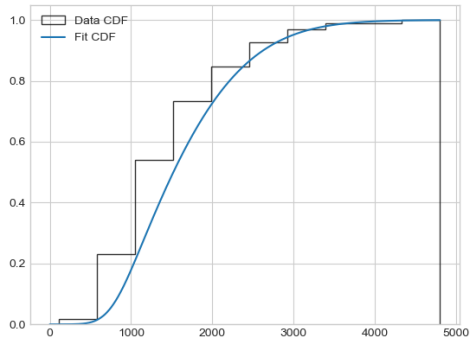

(b) Actual Kolmogorov–Smirnov test of gas consumption of MV/LV station. This CDF corresponds to the PDF of Figure 6.1
. D-value: 0.0313, p-value:0.657

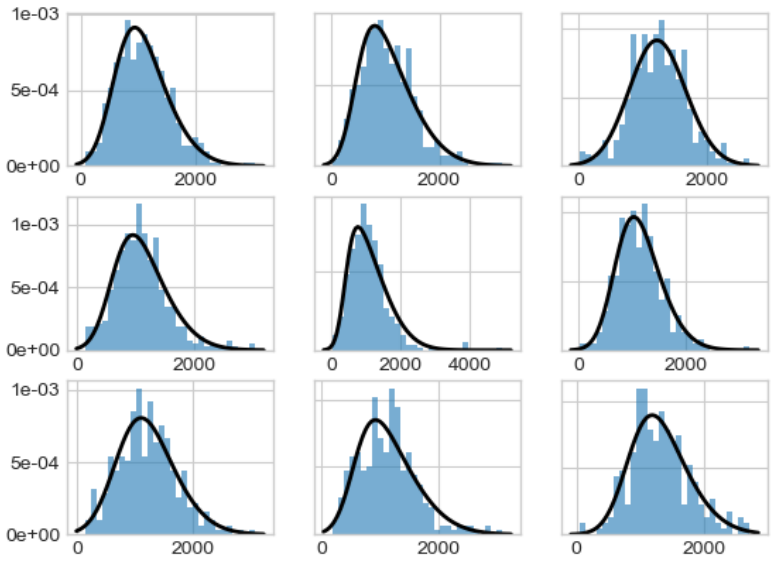

Figure 6.3: Skewed normal distribution fit for the annual gas consumption of 9 of the transformers included in the study in den Bosch. All distributions are highly positively skewed since gas usage is always positive. The K-S test results can be found in Table B.3

6.1 Selecting representative buildings for simulation

Since only the annual consumption of natural gas is known for the buildings connected to the transformer an estimation has to be made as to what buildings are connected to the transformer. In theory, the address data of buildings connected to a transformer could be cross-examined with Basisregistratie Adressen en Gebouwen (BAG) data to identify the year of construction, surface area, and energy labels. Data concerning the type of building (SFH, TH) is not publicly available and is not contained in BAG. It could only be obtained from a third-party data processor as a paid dataset. Furthermore, the Application programming interface (API) of BAG, which is required for a large number of requests such as the city of 's-Hertogenbosch, is not publicly available. Due to time and data availability constraints. A different approach is suggested, which is described in the next two paragraphs.

If all building parameters such as width, length, orientation, window to wall ratio, and story count are known estimating the amount of gas consumption is possible using the method described in section 3.5 with the default values described in that section as well. Heating used for tap water consumption can also be estimated by using occupant estimations in relation to water consumption and energy required for heating this water. Doing the however is impossible because of the many degrees of freedom there are. For this reason for every building in the Tabula dataset, standard annual energy consumption was calculated by taking the default building size. The build year, type of building energy label, and theoretical annual gas consumption of all buildings were logged in a table. Then a sub-selection could be made before a building was chosen. For example, a building that will switch to an electric HP will have an energy label of at least A. Furthermore, only terraced houses and SFHs were included in the search.

Then for each transformer, a set of annual gas consumption quantities were drawn from their corresponding distributions. For each of these, the closest possible default building was matched to it. Then an optimizer would adjust the width and the length of the building to match the gas consumption exactly by keeping reasonable bounds. This was done on the dimensions of the

building since they were the most relevant parameters. A maximum length to width ratio of 3 was chosen to eliminate unrealistic building designs. This was determined by doing a sensitivity analysis the results of which can be seen in Figure 6.4. The window to wall ratio has a very small effect whereas the dimensions have the most effect on energy consumption. A 20% increase in insulation also has quite a large effect. This explains why the effect of the mid-insulated building is the lowest. An example of a set of buildings that were included in the simulation is given in Table 6.1.

Table 6.1: Example of a set of generated representative buildings.

Year	Type	Insulation	width $[m]$	length $[m]$	Gas usage $[m^3a]$	Energy label	kWha/m^2	Trafo ID
2005	SFH	level 1	9.7	10.1	1743	A+	90.0	79.334
2005	SFH	level 1	9.7	10.1	1743	A+	90.0	79.345
1991	TH	level 1	4.9	9.9	1270	A	106.5	79.285
1974	TH	level 2	5.0	10.2	1760	A	147.5	79.285
1974	TH	level 2	5.0	10.5	1760	A	147.5	79.285

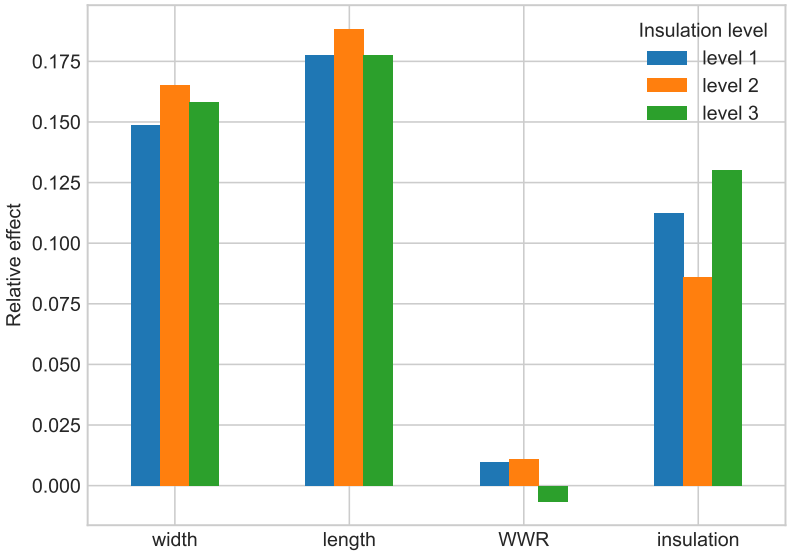

Figure 6.4: Effect of a 20% increase in parameters for all SFHs and THs in the TABULA dataset. The insulation surcharge is defined as an increase in the wall, window, and roof insulation with disregard for the airtightness factor.

6.2 Impact of other trends in the electricity grid

Predictions of transformer based on adding heat pump load profiles to current transformer load profiles say little about the reality if other trends in the power system are not taken into account. Electrification of households means they will from gas-fired cooking to electric cooking, rooftop photovoltaics are installed, and they drive EVs. These technologies will have the most impact on the transformer loading on a household level.

Electric cooking already is the most popular form of cooking in the Netherlands. In 1013 electric cooking held a market share of 45% of all newly sold units, which has been steadily increasing to

82% in 2019 [2]. Therefore it is safe to conclude that this is a relatively mature market that will have a limited effect as compared to heat pumps. Additionally, this research focuses on transformer loading on the demand side, not on the generation side. Therefore a summer analysis, which is outside of the heating season, is excluded. In wintertime, photovoltaic panels do generate some power but this is very small compared to the summer. It is assumed that this effect is negligible compared to the uncertainty in market penetration of heat pumps and EVs.

Electric vehicles however are expected to have a major impact on the electricity grid [33]. Therefore conclusions about the transformer loading when heat pumps are added will not be close to reality if the adoption of EVs is not considered. At the end of 2020, the number of vehicles with a plug was a little over 270.000. This is around 3.1% of the 8.700.000 cars in the Netherlands [33]. The Dutch government wants all vehicles sold after 2030 to have no added carbon emissions [33]. ELAAD, the Dutch research institute for electric vehicles expects EVs to comprise around 25% of all Dutch cars by 2030, but trends in electric mobility are rapidly developing so exact predictions are hard to make [33]. For these case studies, it is therefore assumed that 25% of households will have an EV by 2030.

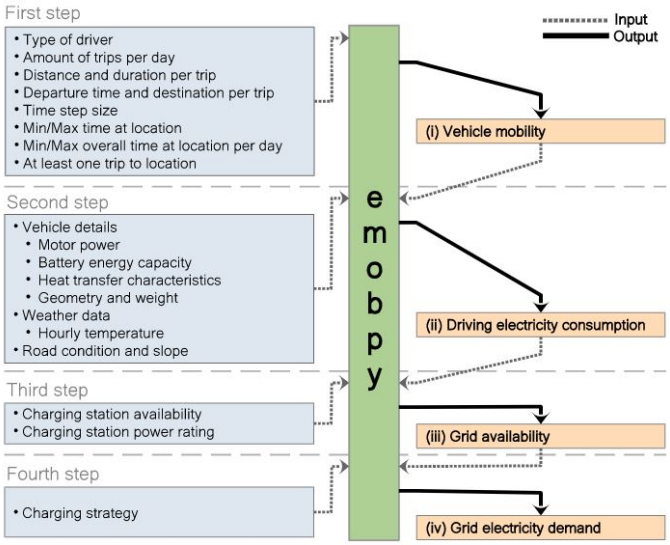

Figure 6.5: Inputs and outputs of emobpy and sequence of generating time series [16].

Modeling the load that EVs will have on transformer loading was done by using work from [16]. He built an open-source tool that is capable of generating EV time series based on empirical data. His approach consists of four steps which can be seen in Figure 6.5. First, a vehicle mobility profile is generated. This is a profile that contains information on the location of a certain vehicle at each point in time. If the vehicle is driving also the distance traveled is saved here. The vehicle mobility profile is generated based on statistics from the comprehensive mobility survey *Mobilität in Deutschland*.

This information is used to calculate the electricity consumption of a certain electric vehicle. The electric vehicle information is taken as all-electric vehicle models that are currently in use. The energy required for every trip is calculated based on the ambient temperature and traction effort for the vehicle's movement. Driving cycles are taken into account to simulate driving. Weather data and vehicle insulation is also used to compute the heating and cooling demands of the vehicle. An example of all losses that an EV experiences and what is taken into account can be seen in the appendix Figure B.2. For this research, it is assumed that all-electric vehicle models have an equal market share. The driving electric consumption profile and the vehicle mobility profile are combined with statistics to provide a grid availability time series. Different charging stations may be available for a vehicle and they are selected based on various probability distributions. These charging stations are assigned charging capacities in accordance with [33].

The last step is generating an actual grid electricity demand time series. This is the important profile for assessing transformer loading. For this research, a slow charging strategy is applied which takes into account the duration a vehicle is connected to a charging station and the energy that is required to fully charge the battery. This allows the battery to be charged at a lower capacity than the maximum capacity that is available for the car and charging station combination.

6.3 Scenario's

To say study the effect of various adoption rates for heat pumps many variables need to be determined or assumed. Therefore scenarios will be sketched which can set these for us and they will be compared to the base case.

The first scenario is a 30 % adoption rate of ASHP. It is assumed that existing buildings will not adopt a GSHP since in an urban area this is usually done on the ground that the building is located upon 4.1.1. This is no longer (financially) possible when the building has been built. In this scenario, no new build buildings are taken into account since it is assumed that new building projects are not going to be connected to existing infrastructure. The adoption rate of 30% is chosen because Enexis presents this as an expected scenario in their investment plans [12]. Nigh time setback temperatures according to Table 5.3 is taken into account in the simulation. Netbeheer nederland, an alliance of the dutch distribution and transmission system operators, wants between 1 and 2 million HHPs installed in the Netherlands by 2030. With roughly 8 million homes in the Netherlands, their pleaded adoption rate would be around 12.5 to 25%. A conservative estimate of 15% HHPs is made for scenario 1.

The second scenario is slightly more extreme. Here it is assumed that full electric heat pumps become the norm. Again the expected adoption rate of 30% is taken as the norm. Scenario 3 is more extreme with an adoption rate of 50% heat pumps. Of these heat pumps, 50% is assumed to be a HHP and the others are ASHPs. For all scenarios, a homogeneous adoption of heat pumps is assumed. Furthermore, a 25% adoption rate of EVs with a homogeneous spread is taken into account for all scenarios. The simulation has also been done without the adoption of EVs. The results can be seen in Appendix B

Table 6.2: Scenario's that might occur in den Bosch

	Scenario 1: expected	Scenario 2: electric	Scenario 3: extreme
HP adoption rate	30%	30%	50%
Types of HP	ASHP, HHP	ASHP	ASHP, HHP
HP power	section 4.7	section 4.7	section 4.7
T setback	Table 5.3	Table 5.3	Table 5.3
Spread of adoption	HHP 50%ASHP 50%	Perfect homogeneous	50% HHP 50%ASHP
EV adoption	25% of households	25% of households	25% of households

6.4 Results

The first step in identifying what the impact of heat pump market penetration on transformers will be is identifying what a transformer overload is. Transformers have a rated capacity but can be overloaded to 130% of their rated capacity for a while without damage to the systems. Currently, this happens quite often due to the high electricity demand occurring from electrification. However, if a transformer is overloaded more than 130 % damage may occur quite quickly and protection mechanisms will disconnect customers from the grid to prevent component damage. This provides the following three categories which are also used in Table 6.3.

1. Black: the load does not exceed the rated capacity of the transformer during the entire simulation period.

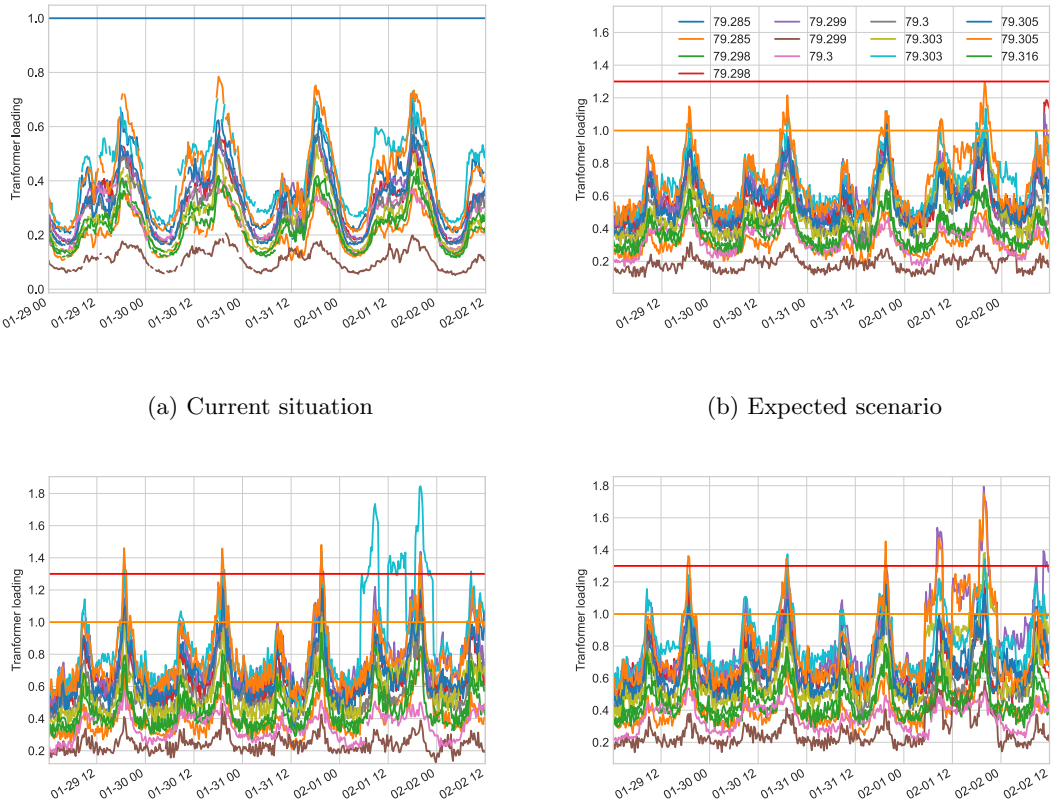

(a) Current situation

(b) Expected scenario

(c) Electric scenario

(d) Extreme scenario

Figure 6.6: Power loading of all transformers. The simulation was done for the entire month of January and February. A snapshot of 29th of January to 2nd of February 12:00 is shown because this was a fairly congested period when the simulation was executed.

2. Orange: The load exceeds the rated capacity but does not exceed 130% of the rated capacity during the simulation period. More than a single measurement is required to eliminate DALI measurement errors.

3. Red: Critical situation where the transformer is overloaded for more than 130%. More than a single measurement is required to eliminate DALI measurement errors.

Providing more than a binary category is also advantageous for Enexis since this makes it easier for them to prioritize investments.

The current situation for the transformer loading on an average winter day can be seen in Figure 6.6a. The loading is defined as the power expressed as a fraction of the specific maximum loading of the transformer. This allows for visualization in a single figure for many transformers. Here the maximum loading of all transformers that is reached is 80% of the maximum load which is reached by transformer 79.298. During the entire winter period, the maximum load reached by any transformer was 85.4% which was reached by transformer 79.328.

The results of expected, electric and extreme scenario can graphically be seen in figures 6.6b 6.6c and 6.6b. The load profiles get more twitchy as heat pump profiles are added. This depends on the specific control strategy that is applied 5.3.

Drastic measurements are needed to prevent extreme overloading of many transformers. In the expected scenario, 6 out of the 13 analyzed transformers are critically overloaded. The most over-

Table 6.3: Number of hours each transformer loading exceeds maximum loading during simulation period with an EV penetration of 25%.

	Expected scenario		Electric scenario		Extreme scenario	
Transformer	100%	130%	100%	130%	100%	130%
79.285	48	11	104	10	135	8
79.298	0	0	0	0	0	0
79.299	0	0	1	0	2	0
79.3	45	5	54	7	81	3
79.303	76	19	218	31	303	34
79.305	0	0	0	0	0	0
79.316	0	0	0	0	5	0
79.317	11	0	24	2	35.5	0
79.327	11	0	10	0	24	4
79.328	162	14	295	47	300	40
79.329	37	10	77	3	78	6
79.334	144	16	327	65	314	41
79.345	3	0	10	0	3	0

loaded transformer is critically overloaded for a duration of 18.5 hours during the winter months (see Table B.2 for maximum transformer loading). The maximum loading of this transformer is 236% of its rated capacity. At this point protection measures start and load shedding occurs. This means part of the customers will be disconnected from the grid and be left in the dark. This is a very undesirable situation. This situation gets worse as the penetration of heat pumps increases. Not only are transformers overloaded for a longer duration and more frequently, but also the magnitude at which they are overloaded increases Figure 6.6 and Table B.2.

Secondly, the difference between the extreme (high) scenario and the expected (low) scenario is not extremely high. In the expected scenario, 6 out of the 13 transformers are critically overloaded which rises to 8 out of 13 for the extreme scenario (an increase of 33%). It seems that the transformers that require reinforcement are independent of the scenario. There was not a single transformer that went from not overloading in the expected scenario, to critical overloading in the extreme scenario. This makes prioritizing investments easier because the confidence in a specific scenario occurring can be lower due to them being less relevant.

The last conclusion can be drawn by observing Table B.1 in Appendix B. This table presents the results of the same scenarios if electric vehicles are not taken into account. Those results seem a lot less dramatic with not a single transformer critically overloading in the expected scenario. Even if the extreme scenario is considered only 3 out of 13 (23%) of transformers are critically overloading with a max load of 143% during the entire winter period. From this, it can be concluded that with few investments, the transformers included in this case study can handle the integration of heat pumps. Large problems only start to occur if EVs are considered.

Chapter 7

Conclusions and discussion

This research set out to assess how the impact of residential heat pump market penetration on the low to medium voltage network can be modeled. After analyzing related work this research question was broken down into five subquestions which together built up to a final model. First, the whole system that was going to be modeled was presented with its variations.

A 4R3C thermal network analogy of a building was developed to mathematically formalize what heat transfer mechanisms occur within a building and how heating will affect this. This was done by drawing an electrical system analogy and rewriting the most important sources of low-temperature heat transfer, conduction and convection, in thermal network analogy form. The effects of ventilation and infiltration were taken into account by using the airtightness of a building and a potential heat recovery fraction from the ventilation system. The effects of solar irradiation were taken into account by taking the intensity of its direct normal irradiance and using a spherical coordinate system to compute the heating intensity. Lastly, the effect of Domestic Hot Water (DHW) was modeled separately from space heating demand. This was done because DHW consumption is a separate system from space heating which requires its own model and mostly depends on occupant behavior.

The building model was made generic and applicable to a wide range of Dutch buildings by using a two-step process. First, the building classification scheme from the TABULA project [26] was used to divide the Dutch residential building stock into age and size classes. This resulted in a set of synthetically generated buildings based on commonly found construction elements en renovation measurements of certain buildings. These buildings represent a wide variety of Dutch buildings of which thermal properties are known. The second step was done in the case study where heat pump market penetration was modeled on transformers in s Hertogenbosch. Measurements of gas annual gas consumption of buildings that are connected to these transformers indicated their thermal demand. Adapting a synthetic building's shape parameters and calculating the effect on annual thermal demand were done by a solver to find the correct model inputs to represent an actual building.

A wide variety of heat pumps were described. Their benefits and drawbacks have been discussed. The most distinctive difference for this research was the effect of Coefficient of Performance (CoP), the ratio between electrical input and thermal output. Air Source Heat Pump (ASHP) are highly affected by the outside temperatures whereas Ground source Heat Pump (GSHP) are not. Correlations from [35] have been used to model the heat pump CoP relations. All heat pumps present in this study used a thermal buffer tank to reduce cycling frequency since a high cycling frequency reduces the lifetime of the heat pump.

In section 4.4 an extensive analysis of heat pump controllers was conducted to study what the effects of various control strategies are on heat pump load profiles. Both single speed and variables speed control methods were researched. However, since the full electric heat pumps present in the study were monovalent, only a bang-bang control could be applied. These profiles were verified in chapter 5. Since a large dataset of variable speed heat pumps was available, the single-speed control strategy was not verified. Two types of the multiple hysteresis control, a Proportional

(P) controller and a Proportional Integral (PI) controller were plotted against measured data. A nighttime setback temperature was introduced since this presented itself in the measured data. In the final analysis, the combined load profiles of a group of heat pumps were compared with each other since this was seen as more relevant on actual transformers, and the effects of random variations are tempered. Eventually, it was concluded that a single control strategy did not perfectly represent measured data. Various manufacturers program their own control algorithms, which are not shared with competitors. It is therefore assumed that a measured dataset will contain multiple control algorithms. Therefore a mix of control multiple hysteresis and PI control strategies should be used.

The effects of various degrees of heat pump market penetration were investigated by simulating three scenarios, expected, electric, and extreme. A differentiation between houses that are connected to various transformers was made by doing a statistical analysis of the annual gas consumption of the buildings that are connected to each transformer. This enabled differentiation between urban and more rural transformers. The load profiles that were generated for each scenario were added to the current transformer loading. The effects of the growing market share of Electric Vehicles (EVs) were accounted for by using work from [16] and expected market adoption of 25% [33]. The simulation was also executed without the integration of EVs. In section 6.4 three conclusions were drawn from this case study. First, drastic measurements are needed to prevent extreme overloading of transformers. In the expected scenario 46% of transformers in the case study experience critical overloading during the simulation period with a maximum loading of 246% of its rated capacity. Second, this is scenario independent. There was not a single transformer that went from not overloading in the expected scenario, to critical overloading in the extreme scenario. Lastly, the transformers are capable of handling the integration of heat pumps if electric vehicles are not considered. If the simulation is run without the adoption of electric vehicles there is no critical transformer overload in the expected scenario. Even in the most extreme scenario, only 23% of the transformers considered are overloading with a max load of 143% during the entire winter period.

7.1 Discussion and limitations

Throughout this research, various assumptions had to be made and some effects are omitted. This results in deviations from reality and leaves recommendations for future work open. The impact that heat pumps will have on the low voltage electricity grid was investigated. This was done by generating load profiles that heat pumps in a certain area might have and adding them to current transformer loads. The conclusions drawn from this analysis implicitly assumed that transformer loading only increases as a result of heat pumps that are added to the electricity grid and excluded other major impacts on the electricity grid such as electric vehicles and distributed electricity generation. Therefore transformers listed in Table 6.3 that are not expected to overload due to heat pumps might still overload when effects from other trends are taken into account.

Furthermore, occupant behavior was only taken into account by introducing nighttime setback temperatures, which could be seen in measurement data. In reality, the impact of human behavior on energy consumption profiles is much more complicated than that. [29] reported the results of a large-scale study on actual versus theoretical energy consumption of buildings in the Netherlands. The study comprised around 200.000 energy labels of Dutch buildings, which were coupled with statistics of actual energy consumption. The labels were computed using the methods described in section 3.5 and were therefore independent of actual energy consumption. Figure 7.1b shows their normalised results. For high-performance buildings, the actual energy consumption is slightly higher than expected whereas in poorly insulated buildings a much higher gas consumption is expected than is measured. This might be an example of the Jevons paradox, where more efficient use of a certain resource will lead to an increase in consumption of the same resource due to falling costs. People with less efficient homes might have lower thermostat settings or leave some rooms (such as bedrooms) unheated.

Heat pump adaptation is modeled according to a homogeneous spread of adoption. This is

likely not correct because of natural adaptation patterns. There are a variety of technical, social, and economic factors that determine whether dwelling owners switch to a heat pump or not. For example level of insulation, ease of installation of a heat pump, and financial situation. Since socio-economic factors are not homogeneously spread it is likely that heat pump adaption is not either. [8] used a spread that was based on interview questions of socioeconomic factors to assign relative probabilities of adaptation to transformers. These interviews, however, were done in different countries where people have different opinions concerning gas-fired heating and heat pumps. In Germany for example the government is actively promoting the transition *towards gas-fired heating* by providing subsidies because gas-fired heating is seen as environmentally friendly [9]. Further research is required to determine how heat pump adaptation will spread in the Netherlands to make a more accurate prediction of future transformer loading.

Adoption of heat pumps is modeled according to current building gas usage, but people who switch to a heat pump are expected to first improve their insulation standards, and then switch to a heat pump. Therefore actual individuals who switch might be skewed to the left of the distribution. However, the results by [29] expressed in total gas consumption per label Figure 7.1a also indicate that from gas consumption alone nothing can be said about the energy label. The edge of the standard deviation of the highest-performing buildings is the mean consumption of the lowest-performing buildings. Was the reason for randomly sampling gas consumption from the whole distribution per transformer as explained in section chapter 6 and not just from the lower bound of the distribution.

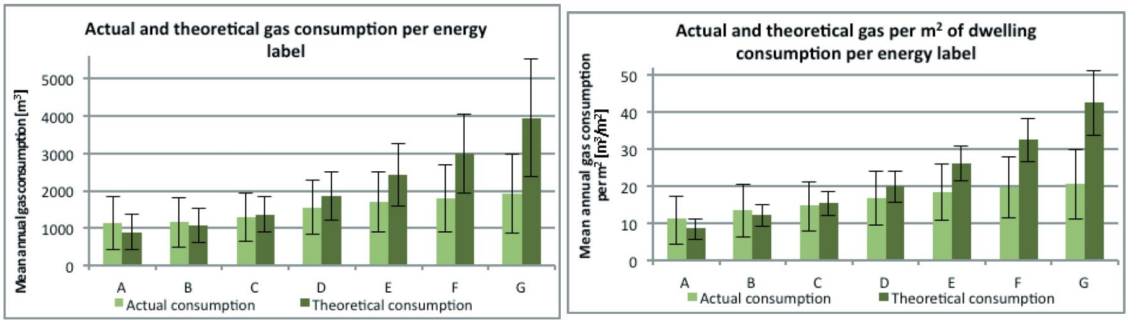

(a) Total

(b) Normalised

Figure 7.1: Actual and theoretical average gas consumption (m3) in dwellings per label category with ±1 standard deviation

The simulation was done in a white box manner where building parameters functioned as the input for the simulation. However many parameters that were used for classification were not publicly available for specific buildings, therefore annual gas consumption was used to select a building that would closely match the parameters set by the building. This however does not utilize the full potential of the model. Future research should try to include this data as a starting point to improve the results.

Additionally, Typical Meteorological Year (TMY) data was used to assess what the impact will be. Therefore the results only show what happens for this specific weather data, which is not an extreme case. If transformer overloading is not predicted for TMY data, it does not guarantee that this will not happen, because TMY data is an average.

Bibliography

[1] Meteorological data. URL https://www.tudelft.nl/en/ewi/over-de-faculteit/afdelingen/electrical-sustainable-energy/photovoltaic-materials-and-devices/dutch-pv-portal/meteorological-data. 18

[2] The statistics portal. URL https://www.statista.com/markets/. 42

[3] Handige info, tips & kosten: 2022. URL https://warmtepomp-weetjes.nl/. 31

[4] Hybrid Heat Pumps Final report for. Technical report, 2017. 3

[5] Window energy efficiency: Solar heat gain and visible transmittance, Aug 2018. URL https://www.glewengineering.com/window-energy-efficiency-solar-heat-gain-and-visible-transmittance/. 11

[6] Open data, Feb 2022. URL https://www.cbs.nl/nl-nl/onze-diensten/open-data. 34

[7] M. Akmal, B. Fox, D. J. Morrow, and T. Littler. Impact of high penetration of heat pumps on low voltage distribution networks. In *2011 IEEE PES Trondheim PowerTech: The Power of Technology for a Sustainable Society, POWERTECH 2011*, 2011. ISBN 9781424484195. doi: 10.1109/PTC.2011.6019401. 22

[8] Raoul Bernards, Johan Morren, and Han Slootweg. Development and Implementation of Statistical Models for Estimating Diversified Adoption of Energy Transition Technologies. *IEEE Transactions on Sustainable Energy*, 9(4):1540–1554, 10 2018. ISSN 1949-3029. doi: 10.1109/TSTE.2018.2794579. URL https://ieeexplore.ieee.org/document/8260957/. 3, 48

[9] Thijs ten Brinck. 'duitse subsidie op aardgas' vooral bij nederlanders bekend?, Mar 2021. URL https://www.wattisduurzaam.nl/32842/energie-beleid/subsidie-stimulering/duitse-subsidie-op-aardgas-vooral-bij-nederlanders-bekend/#:~:text=Daarom%20subsidieert%20Duitsland%20(onder%20voorwaarden,De%20Nederlandse%20voorsprong. 48

[10] John Clauß and Laurent Georges. Model complexity of heat pump systems to investigate the building energy flexibility and guidelines for model implementation. *Applied Energy*, 255, 12 2019. ISSN 03062619. doi: 10.1016/j.apenergy.2019.113847. 19, 22, 26, 34

[11] Tech Controllers. Heating curve - what is it and how to set it? - tech sterowniki, Mar 2020. URL http://tech-controllers.com/blog/heating-curve---what-is-it-and-how-to-set-it. 23

[12] Evert den Boer and Jeroen Sanders. Enexis Netbeheer investeringsplan 2022. Technical report. URL https://www.enexis.nl/-/media/downloads/investeringsplan-en-bijlagen/enexis-netbeheer-investeringsplan-2022.pdf. 43

[13] Matteo Dongellini, Massimiliano Abbenante, and Gian Luca Morini. A strategy for the optimal control logic of heat pump systems: impact on the energy consumptions of a residential building. Technical report, 2017. 25, 27, 33

[14] David Fischer and Hatef Madani. On heat pumps in smart grids: A review, 4 2017. ISSN 18790690.

[15] Sam Foster, Sophie Lyons, and Ian Walker. Hybrid Heat Pumps Final report for Department for Business, Energy & Industrial Strategy. Technical report, 2017.

[16] Carlos Gaete-Morales, Hendrik Kramer, Wolf Peter Schill, and Alexander Zerrahn. An open tool for creating battery-electric vehicle time series from empirical data, emobpy. *Scientific Data*, 8(1), 12 2021. ISSN 20524463. doi: 10.1038/s41597-021-00932-9.

[17] The Hague. Climate Agreement. Technical report, 2019.

[18] Maarten Hommelberg, Guido Janssen, and Paul Friedel. Eindrapportage-Installatiemonitor-v2.1.

[19] Ulrike Jordan and Klaus Vajen. INFLUENCE OF THE DHW-LOAD PROFILE ON THE FRACTIONAL ENERGY SAVINGS: A CASE STUDY OF A SOLAR COMBI-SYSTEM WITH TRNSYS SIMULATIONS. Technical report, 2000.

[20] Ulrike Jordan and Klaus Vajen. DHWcalc: PROGRAM TO GENERATE DOMESTIC HOT WATER PROFILES WITH STATISTICAL MEANS FOR USER DEFINED CONDITIONS. In *ISES Solar World Congress*, Orlando, 2005. URL www.solar.uni-kassel.de.

[21] Philip Kosky, Robert Balmer, and George Wise. *Exploring Engineering*. Elsevier inc, 3 edition, 2013. ISBN 978-0-12-415891-7.

[22] Tuule Mall Kull, Martin Thalfeldt, and Jarek Kurnitski. Optimal PI control parameters for accurate underfloor heating temperature control. *CLIMA*, 2019. doi: 10.1051/e3sconf/2019111010. URL https://doi.org/10.1051/e3sconf/2019111010.

[23] Tuule Mall Kull, Martin Thalfeldt, and Jarek Kurnitski. PI parameter influence on underfloor heating energy consumption and setpoint tracking in NZEBs. *Energies*, 13(8), 4 2020. ISSN 19961073. doi: 10.3390/en13082068.

[24] R. van Leeuwen. *Towards 100% renewable energy supply for urban areas and the role of smart control*. PhD thesis, University of Twente, Enschede, The Netherlands, 5 2017. URL http://purl.org/utwente/doi/10.3990/1.9789036543460.

[25] Tobias Loga and Nikolaus Diefenbach. *Typology Approach for Building Stock Energy Assessment TABULA Calculation Method-Energy Use for Heating and Domestic Hot Water-Reference Calculation and Adaptation to the Typical Level of Measured Consumption-TABULA Documentation-TABULA Project Team*. 2013. ISBN 9783941140318. URL www.iwu.de.

[26] Tobias Loga, Britta Stein, and Nikolaus Diefenbach. TABULA building typologies in 20 European countries—Making energy-related features of residential building stocks comparable. *Energy and Buildings*, 132:4–12, 11 2016. ISSN 03787788. doi: 10.1016/j.enbuild.2016.06.094.

[27] Hatef Madani, Joachim Claesson, and Per Lundqvist. Capacity control in ground source heat pump systems part II: Comparative analysis between on/off controlled and variable capacity systems. In *International Journal of Refrigeration*, volume 34, pages 1934–1942, 12 2011. doi: 10.1016/j.ijrefrig.2011.05.012.

[28] Hatef Madani, Joachim Claesson, and Per Lundqvist. A descriptive and comparative analysis of three common control techniques for an on/off controlled Ground Source Heat Pump (GSHP) system. *Energy and Buildings*, 65:1–9, 2013. ISSN 03787788. doi: 10.1016/j.enbuild.2013.05.006.

[29] Daša Majcen, Laure Itard, and Henk Visscher. Energy labels in Dutch dwellings-their actual energy consumption and implications for reduction targets. In *CLIMA*, pages 1947–1957, 2013.

[30] Netbeheer Nederland. Brede coalitie pleit voor 1 miljoen hybride warmtepompen. URL https://www.netbeheernederland.nl/nieuws/brede-coalitie-pleit-voor-1-miljoen-hybride-warmtepompen--1453.

[31] Danny S Parker and Philip W Fairey. Estimating Daily Domestic Hot-Water Use in North American Homes 2015 ASHRAE Conference. Technical report, 2015. URL http://www.ashrae.org.

[32] PBL Planbureau voor de Leefomgeving. Startanalyse aardgasvrije buurten (versie 2020, 24 september 2020); Gemeenterapport met toelichting bij tabellen met resultaten van de Startanalyse. Technical report. URL www.expertisecentrumwarmte.nl/contact.

[33] Nazir Refa, Daan Hammer, and Jan van Rookhuyzen. Elektrisch rijden in stroomversnelling. Technical report, ELAAD, 2021.

[34] Reinoud Segers, Robin Niessink, Robin van den Oever, and Marijke Menkveld. Warmtemonitor 2019.

[35] Oliver Ruhnau, Lion Hirth, and Aaron Praktiknjo. Time series of heat demand and heat pump efficiency for energy system modeling. *Scientific Data*, 6(1), 12 2019. ISSN 20524463. doi: 10.1038/s41597-019-0199-y.

[36] Pamela Vocale, Gian Luca Morini, and Marco Spiga. Influence of outdoor air conditions on the air source heat pumps performance. In *Energy Procedia*, volume 45, pages 653–662. Elsevier Ltd, 2014. doi: 10.1016/j.egypro.2014.01.070.

[37] Joakim Widén, Magdalena Lundh, Iana Vassileva, Erik Dahlquist, Kajsa Ellegård, and Ewa Wäckelgård. Constructing load profiles for household electricity and hot water from time-use data—modelling approach and validation. *Energy and buildings*, 41(7):753–768, 2009.

[38] Karl Zandi. How are single-family and multi-family buildings defined? URL https://www.economy.com/support/blog/buffet.aspx?did=8015A9FA-79EF-4EE6-BF79-C84EC932B331.

[39] Xiang Zhang, Ernst Gockenbach, Volker Wasserberg, and Hossein Borsi. Estimation of the lifetime of the electrical components in distribution networks. *IEEE Transactions on Power Delivery*, 22(1):515–522, 1 2007. ISSN 08858977. doi: 10.1109/TPWRD.2006.876661.

Appendix A

Model assumptions

Table A.1: Assumptions for the building, heat pump and simulation

Unit	value	Unit	value
Cold tap water	15 °C	Indoor temperature	20 °C
Convective heat transfer	10 $W/(m^2K)$	Internal generation	3 W/m^2
Floor material	Concrete	Max floor power	100 W/m^2
Floor thickness	10 cm	Period	Jan 1 - March 1
Ground temperature	15 °C	Ventilation schedule	24/7 on
Heat recovery (if applicable)	70%	Water in underfloor heating	1,2 L/m^2
Hot tap water	40 °C	Weather	TMY data

Appendix B

Additional case study details

B.1 Additional results and details

Table B.1: Number of hours each transformer loading exceeds maximum loading during simulation period without EVs.

	Scenario 1		Scenario 2		Scenario 3	
Transformer ID	100%	130%	100%	130%	100%	130%
79.285	0	0	17	0	28	0
79.298	0	0	0	0	0	0
79.299	0	0	0	0	0	0
79.3	0	0	4	0	6	0
79.303	0	0	22	1	44	1
79.305	0	0	0	0	0	0
79.316	0	0	0	0	0	0
79.317	0	0	2	0	1	0
79.327	0	0	0	0	1	0
79.328	5	0	49	0	98	1
79.329	0	0	7	0	5	0
79.334	10	0	98	2	120	2
79.345	0	0	0	0	0	0

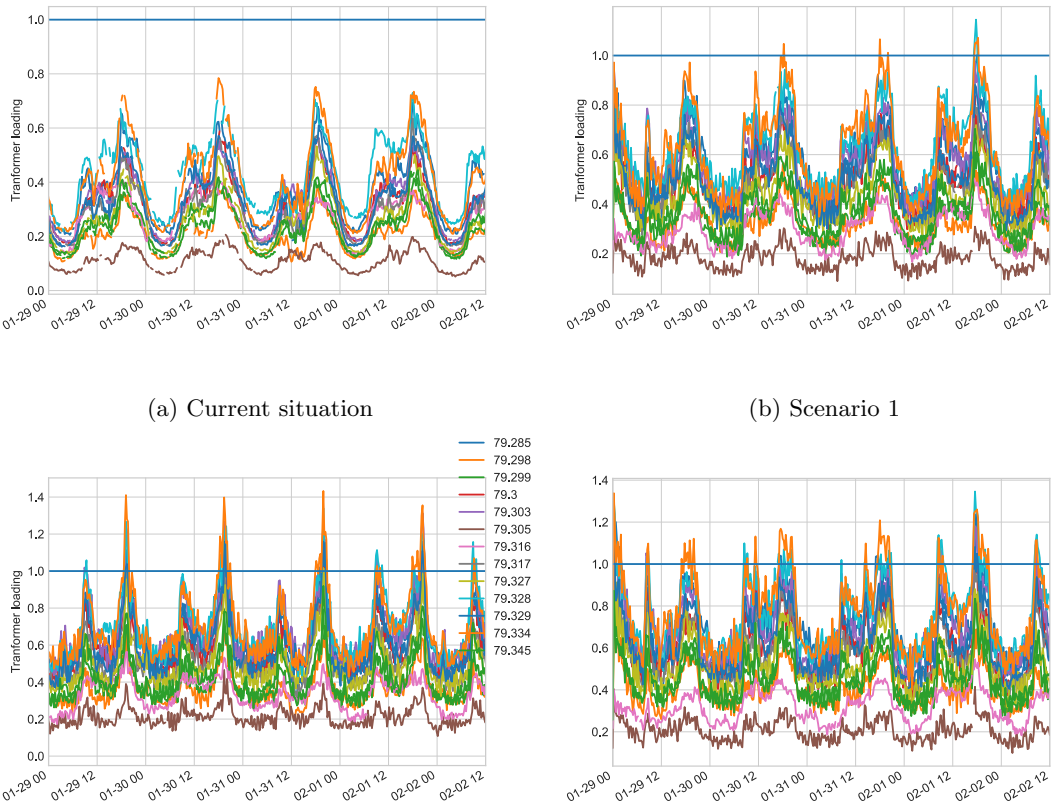

(a) Current situation

(b) Scenario 1

(c) Scenario 2

(d) Scenario 3

Figure B.1: Power loading of all transformers with heat pumps but no Electric Vehicle. The simulation was done for the entire month of January and February. A snapshot of 29th of January to 2nd of February 12:00 is shown because this was a fairly congested period when the simulation was executed.

Table B.2: Maximum overload of transformers during simulation period. Because this is a single peak during a period of 2 months this value should not be read on its own to draw conclusions. Transformer 79.303 for example has a peak loading in the expected scenario than in the electric scenario (with EV). The overloading Table 6.3 however shows that this transformers critically overloading duration is almost twice as high.

	With EV			Without EV		
Transformer	Expected	Electric	Extreme	Expected	Electric	Extreme
79.285	1.81	1.63	1.77	1.02	1.21	1.2
79.298	0.89	1.0	1.01	0.56	0.78	0.71
79.299	1.0	1.04	1.11	0.62	0.79	0.81
79.3	1.5	1.61	1.55	0.91	1.14	1.14
79.303	2.36	1.76	1.79	0.95	1.31	1.33
79.305	0.64	0.71	0.72	0.31	0.47	0.4
79.316	0.85	0.74	1.29	0.53	0.56	0.57
79.317	1.13	1.41	1.32	0.83	1.06	1.09
79.327	1.22	1.34	1.54	0.77	1.02	1.04
79.328	1.91	2.28	2.25	1.11	1.34	1.35
79.329	1.54	1.51	1.43	1.02	1.16	1.17
79.334	1.89	2.05	1.8	1.15	1.43	1.43
79.345	1.17	1.28	1.2	0.68	0.92	0.88

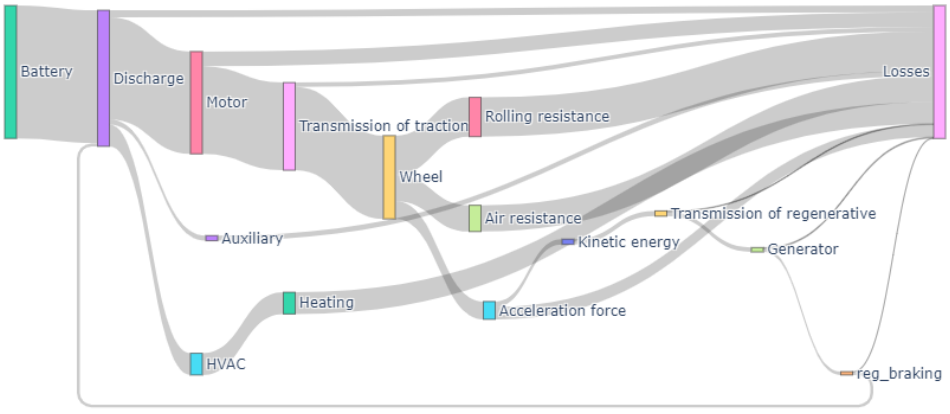

Figure B.2: Example of losses that a Volkswagen ID3 experiences in January.

B.2 Statistics

Table B.3: KS statistics of the transformers seen in figure 6.3. Location of the results matches the location of the sub figures.

Figure		1	2	3
	skew	2.25	3,23	0,81
	loc	589	447	984
1	scale	671	776	506
	D-value	0,031	0,036	0,03
	P-value	0,66	0,63	0,85
	skew	2,35	4,17	1,97
	loc	612	396	714
2	scale	676	893	610
	KS	0,048	0,074	0,029
	P-value	0,32	0,033	0,92
	skew	1,76	2,9	2,05
	loc	719	556	831
3	scale	709	770	664
	KS	0,028	0,051	0,034
	P-value	0,96	0,38	0,92